Physics – Uspekhi **44** (4) 397 – 414 (2001)

REVIEWS OF TOPICAL PROBLEMS PACS numbers: **07.68.+m**, 71.35.Cc, **82.50.–m**

Exciton photochemistry of light-sensitive crystals

B U Barshchevskiĭ

DOI: 10.1070/PU2001v044n04ABEH000931

Contents

1. **Introduction** 397
2. **Hydrogen-like properties of photochemical and impurity color centers in metal halides** 397
3. **Temperature dependence of the light sensitivity of unsensitized photographic materials and of photographic materials with heavy-metal compounds as impurities** 407
4. **Conclusions** 413

References 414

Abstract. It is shown that in photosensitive materials light absorption centers and centers of latent and developed photographic images are of a hydrogen-like nature, and the light sensitivity together with the photoelectric current have an Uhrbach-type temperature dependence.

1. Introduction

In this review it is shown that the spectra of absorption, photocurrent luminescence, and photochemical (photographic) sensitivity of a number of light-sensitive materials with photochemical and impurity color centers (including silver halides) are hydrogen-like. The proof of this has been obtained with the aid of the theory of excitons, including modified Wannier – Mott equations (for large-radius excitons).

In light-sensitive crystals, the energy levels of the Wannier – Mott excitons are the series limits of spectral lines. The lines and bands in spectra determined for one crystal can be used to find the equivalent characteristics for other crystals via what is known as the correction factor $\varepsilon_2^2/\varepsilon_1^2$, where ε is the dynamic dielectric constant of the corresponding crystals.

The review also studies the temperature dependence of the light sensitivity of photographic materials at the moment of exposure and the effect of compounds of metals with different valences on the light sensitivity of photographic materials deposited on various substrates at room and elevated temperatures. Our analysis demonstrates the possibility to vastly reduce the silver content in silver halide photographic materials and retain the properties of these materials by introducing sodium tungstate into the photographic emulsion. Using this method makes it possible to save about 20 – 30% of silver in some photographic materials and keep the same level of sensitivity. It has been established that sodium tungstate produces an effect on photographic materials only at the exposure stage when the latent photographic image is formed.

B U Barshchevskiĭ N S Kurnakov Institute of General and Inorganic Chemistry
Leninskiĭ prosp. 31, 117907 Moscow, Russian Federation
Tel. (7-095) 952-07 87

Received 27 December 2000
Uspekhi Fizicheskikh Nauk **171** (4) 415 – 433 (2001)
Translated by E Yankovsky; edited by A Radzig

2. Hydrogen-like properties of photochemical and impurity color centers in metal halides

This section discusses the photochemical properties of silver, gold, thallium, and lead halides and alkali halide crystals. Among the above chemical compounds (semiconductors), the most popular in industry are silver halides — their consumption amounts to several thousand tons. In the absence of light they are insulators. The dark conduction in them is ion – electron in nature. Under photochemically active radiation, the silver halide crystals decompose into silver and haloid. At the base of this process lies the photoelectric act which leads to the transformation of halogen ions into halogen and silver ions into neutral silver. The transition of a photoelectron from a halogen ion to a silver ion occurs both through the conduction band and through the formation of excitons which break up at crystal surfaces, phonons, structure imperfections, point defects, and impurities.

Silver halides in light-sensitive materials are in the form of microcrystals of different sizes (from hundredths of a micrometer and larger) depending on the purpose for which the specific material is used, and constitute the main fraction of these materials. The further progress of modern photography and cinematography is inseparable from the use of silver halides.

The development of the theoretical foundation of the photographic process, starting with the theory of latent-image formation, always lagged behind the practical bases of photography, whose progress has been remarkable. The theory of Wannier – Mott excitons [1 – 4] contributed greatly to the understanding of the various processes that take place in the formation of latent-image centers. The basic equation of the Wannier – Mott theory describes the formation in a crystal of a hydrogen-like absorption and emission spectra of light. The energy levels in this crystal are given by the equation

$$\hbar\omega_n = E_g - \frac{e^4\mu}{2\hbar^2\varepsilon^2 n^2}\,, \qquad (1)$$

where $\hbar\omega_n$ are the photon energies corresponding to the lines of excitonic absorption for different values of the quantum number n; E_g is the band gap; $e^4\mu/2\hbar^2\varepsilon^2n^2$ at $n = 1$ is the binding energy of an exciton in the ground state, equal to $R'hc$, with R' being the Rydberg constant for an exciton, and μ the reduced exciton mass.

In order to be able to apply equation (1) to light-sensitive crystals, we use our experimental values of $\hbar\omega_n$, E_g, and ε. To this end, as shown in this section, we can employ the experimental data not only for the position of the maxima of light absorption but also for the position of the maxima of the photocurrent caused by dissociation of Wannier – Mott excitons, and for luminescence due to annihilation of these excitons. Kozyreva and Meĭklyar [5] showed how it is possible to use luminescence data in this case.

To find $R'hc$ for silver halides, we used the values of $\varepsilon = \bar{n}^2$, where $\bar{n}$ is the refractive index determined from the reflectance spectrum through the use of the Fresnel formula. For instance, for AgBr at room temperature and light with $\lambda = 430$ nm we have $\varepsilon = 5.3$, while for AgCl we have the same value of ε at $\lambda = 390 - 400$ nm. For such values of ε we have (for AgBr and AgCl) $R'hc = 0.24$ eV. According to our photoelectric measurements [4], for AgBr at room temperature $E_g = 3.05$ eV. Then the photon energy equal to 2.81 eV and corresponding to the absorption line at $n = 1$ coincides with the value obtained from studying the absorption spectra. When such a photon is absorbed, an electron is transferred almost to the bottom of the conduction band (from the side of the forbidden band), which makes it possible to assume that such Wannier – Mott excitons can dissociate at room (or even lower) temperatures. For an exciton with $n = 2$, we have $\hbar\omega_2 = 2.99$ eV. Such a state is unlikely to exist at room temperature [6].

A similar picture emerges for AgCl at $n = 1$: according to the experimental data on the photocurrent at room temperature we have $E_g = 3.25$ eV and $R'hc = 0.24$ eV. Then $\hbar\omega_1 = E_g - R'hc = 3.01$ eV falls almost at the bottom of the conduction band. Hence, the peak in the photocurrent corresponding to an exciton with $n = 1$ merges with the peak in the photocurrent corresponding to $\lambda = 365$ nm, which represents band-to-band transitions. The reduction of the temperature to -53° makes it possible to separately observe these peaks in the photocurrent [7, 8].

Kozyreva and Meĭklyar [5] discovered line spectra of edge luminescence in AgBr at 4.2 K; they observed a convergent series that consisted of four lines (20631, 21141, 21321, and 21404 cm^{-1}) and could be described by the formula $\nu_n = \nu_\infty - R'/n^2$, where n is equal to 2, 3, 4, and 5, respectively; $\nu_n = 1/\lambda_n$ is the wave number; $\nu_\infty = 21155\,cm^{-1}$, and according to our calculations $R' = 3686$ cm^{-1}. Assuming that these lines correspond to a Wannier–Mott exciton, we obtain $R'hc = 0.46$ eV, which differs from the value of 0.24 eV obtained from photoelectric data at room temperature. This discrepancy is removed by taking into account the temperature dependences of ε and E_g. For AgBr, the temperature coefficient of the dielectric constant, $\varepsilon^{-1}\,d\varepsilon/dT$, is equal to 8.9×10^{-4} K^{-1} [9]. The lowering of the temperature from 297 to 4 K corresponds to a decrease in ε by 27%. Then the value $\varepsilon = 3.9$ correlates with $R'hc = 0.455$ eV, which is almost the value calculated from the above edge luminescence data.

Thus, equation (1) can be employed to describe not only the positions of the maxima in absorption but also the positions of the maxima in photocurrent and the edge-luminescence line spectrum. Taking into account the increase of E_g in AgBr as the temperature drops ($E_g = E_0 - \alpha T$, where $\alpha = 10^{-4}$ eV K^{-1} was obtained from the experimental data of Brown et al. [10] extrapolated to the temperature interval from 300 to 77 K), we get $\Delta E_g = 0.03$ eV. Then the ground state of the exciton at 4.2 K corresponds to the line $\hbar\omega_1 = 3.08 - 0.46 = 2.62$ eV ($\lambda = 472.5$ nm). For $n = 2$, we have $\hbar\omega_2 = 2.965$ eV ($\lambda = 417.5$ nm). According to Kozyreva and Meĭklyar [5], these two lines are observed in the edge luminescence spectrum; they are 0.345 eV apart.

Equation (1) implies that

$$0.345 = \frac{13.6\mu}{\varepsilon^2 m_e}\left[\left(\frac{1}{1}\right)^2 - \left(\frac{1}{2}\right)^2\right],$$

and the reduced exciton mass expressed in units of electron mass is $\mu/m_e = 0.5$.

It is also known that in AgBr at room temperature, maxima in the photocurrent have been observed for wavelengths corresponding to 430 and 460 nm [9]. These maxima are 0.18 eV apart in energy. Then equation (1) also yields $\mu = 0.5m_e$. This result indicates that μ is temperature independent. The line $\lambda = 461$ nm corresponding to the series limit ν_∞ at 4.2 K has not been observed. Note that according to Brown et al. [10], the spectral characteristic of the photocurrent obtained at 2 K exhibits only a step instead of a peak corresponding to $\lambda = 461$ nm, while the peak in the photocurrent at 430 nm is clearly visible, and Kozyreva and Meĭklyar [5] observed the corresponding line in the luminescence spectrum at 4.2 K.

At the self-absorption edge, the positions of absorption peaks, photocurrent maxima, and the convergent series in the line luminescence spectra for AgBr are described by the formula (1) for the Wannier – Mott exciton. It is also known that the photocurrent and the photosensitivity of AgBr, AgCl, and AgI reduce dramatically for light belonging to the excitonic absorption range as the temperature is lowered appropriately, and become very weak at temperatures close to absolute zero [11]. What should be considered the main reason for this phenomenon is the low probability of the exciton dissociation on phonons and a fall in the diffusion rate of the emerging photoelectrons as the temperature goes lower.

More in-depth results have been obtained in studies of edge emission of radiation by AgI crystals. It was found that the bulk of the lines in the edge luminescence spectrum can be obtained through calculations based on a modified version of the equation describing the Wannier – Mott excitons on the assumption that each exciton energy level is the series limit of spectral lines. This equation can be written as follows

$$h\nu' = (E_g - iR'hc) - \frac{R'hc}{n^2}, \qquad (2)$$

where $h\nu'$ are the photon energies corresponding to the lines of excitonic absorption and resonance emission, E_g is the band gap with allowance for the temperature of the crystal, $E_g - iR'hc$ is the series limit, and i is a number characterizing the energy level of an exciton.

Exciton annihilation at low temperatures (e.g. liquid-helium temperatures) is the main process that leads to edge luminescence, since the almost total absence of thermal lattice vibrations excludes dissociation of excitons.

Equation (2) makes it possible to calculate the lines of absorption and resonance emission in γ-AgI, which were observed by Perny [12] at 4.2 K and Lider and Novikov [7] at 4.2 and 77 K. The second paper contains a table with more than 30 luminescence lines in the wavelength range from 419.9 to 460.1 nm (from 23816 to 21734 cm^{-1}, respectively) and describes the position of several lines and bands with shorter wavelengths.

In calculating the wave numbers $\nu_n = 1/\lambda_n$, we used the value $E_g = 3.023$ eV ($E_g/hc = 24289$ cm^{-1}), which is almost the value obtained earlier from the photoelectric data, $E_g = 3.02$ eV, and the value $R' = 1790$ cm^{-1} ($R'hc = 0.222$ eV) obtained from Perny's experimental data [12].

Here are the results of my calculations that use equation (2) rewritten for wave numbers (cm^{-1})

$$\nu_{in} = \left(\frac{E_g}{hc} - iR'\right) - \frac{R'}{n^2},$$

and their comparison with the experimental data obtained by Perny [12] and partially by Lider and Novikov [7].

(1) The values of $\nu_{in} = E_g/hc - R'/n^2 = 24289 - 1790/n^2$ for $i = 0$ are listed in Table 1.

(2) The values of $\nu_{in} = (E_g/hc - R'/2^2) - R'/n^2$ for $i = (1/2)^2$ are listed in Table 2.

(3) At $i = (1/3)^2$ we arrive at the Perny – Lider – Novikov series (the lines corresponding to $n = 3, 4, 5$, and ∞ were observed by Perny [12], while the lines corresponding to $n = 2, 6, 7$, and 8 were discovered by Lider and Novikov [7]) $\nu_{in} = (E_g/hc - R'/3^2) - R'/n^2$ (see Table 3).

(4) The values of $\nu_{in} = (E_g/hc - R'/4^2) - R'/n^2$ for $i = (1/4)^2$ are listed in Table 4.

(5) The values of $\nu_{in} = (E_g/hc - 8R'/9) - R'/n^2$ for $i = 1 - (1/3)^2$ are listed in Table 5.

According to Perny [12], the lines with $n = 2$ and 3 belong to a group of seven equidistant lines with a difference in the wave numbers between the neighboring members of the group equaling 128 ± 2 cm^{-1}. Lider and Novikov [7] assumed that Perny [12] also observed this group of lines, but for the frequency difference he obtained the value of 135 cm^{-1} and the lines were shifted by 2.5 nm. According to our data, the lines observed by Perny [12] belong to the series with different values of i; in addition to a given series with $i = 1 - (1/3)^2$, three lines enter into the series with $i = 1 - (1/6)^2$: 22115 cm^{-1} (452.2 nm), 22372 cm^{-1} (446.9 nm), and 22502 cm^{-1} (444.4 nm). We were unable to reproduce the equidistant group of lines observed by Brown et al. [10], except for the line with 448.7 nm (22286 cm^{-1}) with a discordance of 14 cm^{-1}.

(6) The values of $\nu_{in} = (E_g/hc - R') - R'/n^2$ for $i = 1$ are listed in Table 6.

Table 1.

n	1	2	3	4	5	6	7	8	∞
ν_{in}, cm^{-1} (theory)	22499	23840	24090	24177	24218	24239	24253	24262	24289
ν_{in}, cm^{-1} (expt.)	22502	23832	24090	24189	Band with center at 24242 ± 48				24289
λ_n, nm	444.4	419.7	413.4	412.4					411.8

Table 2.

n	1	2	3	4	5	6	7	8	∞
ν_{in}, cm^{-1} (theory)	22051	23393	23642	23728	23770	23791	23805	23814	23840
ν_{in}, cm^{-1} (expt.)	22045	Undetected	23650	23722	23775	23797	Undetected	23816	23832
λ_n, nm	450 Broad band	Undetected	422.7	421.5	420.8	420.2	Undetected	419.9	419.5

Table 3.

n	1	2	3	4	5	6	7	8	∞
ν_{in}, cm^{-1} (theory)	22300	23642	23891	23978	24018	24040	24054	24062	24090
ν_{in}, cm^{-1} (expt.)	22286	23630	23891	23975	24021	24040	24054	24062	24090
λ_n, nm	447.8	427.0	418.5	419.2	416.2	415.9	415.7	415.5	415.1

Table 4.

n	1	2	3	4	5	6	7	8	∞
ν_{in}, cm^{-1} (theory)	22387	23729	23978	24065	24106	24127	24141	24150	24177
ν_{in}, cm^{-1} (expt.)	22372	23722	23975	Band with center at 24056 (415.7 nm)			Band with center at 24242 (412.4 nm)		
λ_n, nm	446.9	421.5	417.1	Half-width ~ 1.2			Half-width ~ 1		

Table 5.

n	1	2	3	4	5	6	7	8
ν_{in}, cm^{-1} (theory)	20907	22249	22498	22585	22619	22647	22661	22670
ν_{in}, cm^{-1} (expt.)	Undetected	22242	22502	22600		22650	Undetected	
λ_n, nm	478.2	449.6	444.4	442.5		441.5	441.2	441

Table 6.

n	1	2	3	4	5	6	7	8	∞
ν_{in}, cm^{-1} (theory)	20709	22051	22300	22387	22428	22463	22472	22472	22499
ν_{in}, cm^{-1} (expt.)	Undetected	22045	22286	22372		Undetected			22502
λ_n, nm		450 Broad band	448.7	446.9					444.4

The results of the calculations for $i = (1/5)^2$ show that at $n = 2$ they coincide with the experimental data (23770 and 23765 cm^{-1}, respectively), while the other lines fall into broad bands.

For $i = (1/6)^2$ with $n > 3$, all the lines fall into broad bands whose centers are at 24056 cm^{-1} (415.7 nm) and 24242 cm^{-1} (412.4 nm) and whose half-widths are roughly 1.2 – 1 nm.

From our viewpoint, the broad band with its center at 24242 cm^{-1} consists of a very large number of poorly resolved lines belonging to the end members of several series with small values of i and with $n = 5, 6, \ldots$ The edge of this band resides at $h\nu' = E_g = 3.023$ eV (24289 cm^{-1}).

Our calculations have shown that the same phenomenon should be observed in AgBr and AgCl crystals. Kozyreva and Meĭklyar [5] have found such broad bands in these crystals.

Thus, the studies of the spectra for AgI, AgBr, and AgCl based on equations (1) and (2) have revealed that in these crystals the edge-luminescence line spectra differ quantitatively in the values of E_g, R', and i.

The fact that the results of calculations of edge luminescence spectra coincide with the experimental data on AgI prompted researchers to assume that the partial and complete separation of the structures of the AgBr and AgI crystals is the reason why AgBr crystals with an admixture of 1 mol.% AgI exhibit numerous relatively weak lines characteristic of pure AgI (this was discovered by Kozyreva and Meĭklyar [5]).

Silver halides AgHal in the form of fine-grained layers and single crystals are the most universal indicators and detectors of electromagnetic and corpuscular radiation. The injection of certain metals (as impurities) into AgHal crystals was found to result in the emergence of additional absorption bands, photoeffect, luminescence in the visible and red regions of the spectrum and even improved the photographic properties of these crystals [13]. At liquid-helium temperatures, AgHal exhibits absorption spectra caused by injection, as impurities, of positive ions (Cu^{2+}, Ag^{2+}, and Cd^{2+}) or of negative ions (I^- and Cl^-). Kanzaki et al. [14] described the absorption of light by AgCl crystals with copper ions as an impurity at 4.2 K. Such absorption was found to be induced, over a very broad spectral region, by photons whose energies were smaller than the band gap E_g. A copper ion introduced into AgCl (see Fig. 1) represents, as Moser et al. [15] believe, a localized hole which, precipitating near a silver ion in the lattice, is transformed into an ion bound in the form of a molecular complex $(AgCl_6)^{4-}$.

As the temperature is increased to room temperature, the complexes become transformed into $(CuCl_6)^{4-}$. Kanzaki et al. [14] came to this conclusion by employing the results of Moser et al. [15], who used the EPR method and showed that the injection of chalcogens (S, Se, and Te) into the crystal results in the formation of Ag^{2+}-centers. These centers had a broad absorption band corresponding to them with its maximum at about 1.1 eV ($\lambda = 1120$ nm). According to Moser et al. [15], another specific feature of $(AgCl_6)^{4-}$ complexes is light absorption, which forms a band from 2.5 to 0.6 eV, with the maximum in the 1.1 – 1.2-eV range.

Kanzaki et al. [14] studied AgCl crystals purified by floating-zone method and discovered that when such crystals were irradiated by light with $\lambda = 325 - 400$ nm, which corresponded to the principal and the excitonic absorption, a broad absorption band emerged coinciding with the long-wavelength segment of the curve in Fig. 1. The injection of

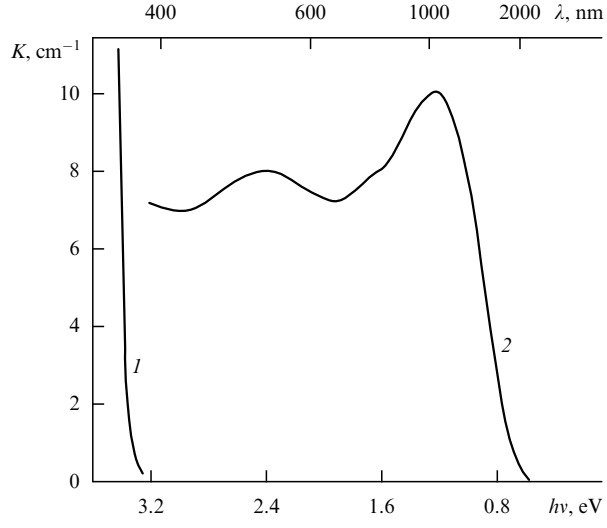

Figure 1. Induced absorption in the $AgCl - Cu^{2+}$ crystal. Irradiation and measurement took place at 4.2 K. Curve *1* represents light absorption in pure AgCl, curve *2* represents light absorption in $AgCl - Cu^{2+}$ after 10-minute irradiation by light whose wavelength is in the 400 – 500-nm range; the concentration of Cu^{2+} is 5×10^{17} cm^{-3}, and the crystal is 3-mm thick [15].

cadmium ions (Cd^{2+}) into these crystals also leads to the formation of an absorption band that differs only slightly from the long-wavelength band induced in pure AgCl.

Comparing the long-wavelength absorption bands referred to in papers [14–16], we see that irrespective of the type of ions injected into the crystal, the position of the absorption bands and their maxima within the spectral characteristics changes little.

Making a similar comparison with the experimental data on $AgCl-Cu^{2+}$ crystals, we see that the wide portion of the induced absorption band in the 3.0–2.0-eV range (410–620 nm) with the maximum at 2.5 eV (496 nm) (see Fig. 1) corresponds to the luminescence band observed in refinely pure AgCl at 2 K [14]. Earlier such a band was observed by Meidinger [17] at 90 K in pure AgCl under exciting radiation with an energy of 3.38 eV (366 nm), and by Belous and Golub [18, 19] in an annealed AgCl crystal.

Figure 1 shows that the third portion of the induced-absorption curve extends from 2.9 eV to the very edge of the fundamental absorption band (~ 3.3 eV). A luminescence band extending to this region of the spectrum has also been observed.

We assume that the above experimental facts can be explained by the laws that characterize heavy hydrogen-like centers or, in other words, 'localized' excitons.

Earlier we noted that the positions of the maxima of photographic (photochemical) sensitivity, photocurrent, and light absorption at the self-absorption edge for AgCl at room temperature is described by equation (1). By employing the modernized Wannier–Mott equation in the case of low temperatures we were able to calculate a considerable fraction of the observed luminescence and absorption lines [20, 21].

As noted earlier, to determine $R' = 2\pi\mu e^4/\varepsilon^2\hbar^2$, we used the high-frequency values of $\varepsilon = \bar{n}^2$.

Heavy-metal impurities in the form of Cu^{2+}, Cd^{2+}, Ag^{2+}, and other ions can be interpreted as singly charged impurities with respect to the crystal lattice with $Z = 1$. When light is absorbed by the crystal, such ions may become hydrogen-like systems with m_e^* (the effective electron mass) much smaller than m_h^*. The reduced mass μ of such a system equals m_e^*, and hence the Rydberg constant R'' is equal to $2R'$. For AgCl crystals we have $R'hc = 0.4970$ eV (4010 cm^{-1}), $R''hc = 0.994$ eV, and $E_g = 3.382$ eV (27280 cm^{-1}) [19, 20].

Below we list the results of calculations for hydrogen-like impurities in AgCl (eV, nm).

In the series $h\nu_{in} = E_g - R''hc/n^2 = 3.382 - 0.994/n^2$ we have lines with $h\nu_1 = 2.39$ (520), $h\nu_2 = 3.13$ (396), $h\nu_3 = 3.27$ (378), $h\nu_4 = 3.32$ (373), $h\nu_5 = 3.34$ (371), $h\nu_6 = 3.35$ (370), and $h\nu_\infty = 3.382$ (366). All calculated lines fall within the absorption bands of Fig. 1, and the line $h\nu_1$ falls into the luminescence bands described by Meidinger [17] and Golub [18]. Furthermore, they fall within the absorption band of AgCl : I [23]

In the series $h\nu_{in} = (E_g - R''hc) - R''hc/n^2 = 2.39 - 0.994/n^2$ we have lines with $h\nu_1 = 1.38$ (899), $h\nu_2 = 2.14$ (580), $h\nu_3 = 2.28$ (542), $h\nu_4 = 2.33$ (531), $h\nu_5 = 2.35$ (527), and $h\nu_6 = 2.36$ (524). These lines fall into the absorption bands of Fig. 1 and the luminescence bands described in Refs [14–19, 22].

In the series $h\nu_{in} = (E_g - R''hc/2^2) - R''hc/n^2$ we have lines with $h\nu_1 = 2.14$ (580), $h\nu_2 = 2.88$ (430), $h\nu_3 = 3.02$ (412), $h\nu_4 = 3.07$ (410), $h\nu_5 = 3.09$ (408), and $h\nu_6 = 3.10$ (406) which fall into the absorption band of Fig. 1 and the luminescence band described by Meidinger [17].

In the series $h\nu_{in} = (E_g - R''hc/3^2) - R''hc/n^2$ we have lines with $h\nu_1 = 3.27 - 0.994 = 2.28$ (542), $h\nu_2 = 3.02$ (411), $h\nu_3 = 3.16$ (391), $h\nu_4 = 3.21$ (386), $h\nu_5 = 3.23$ (385), and $h\nu_6 = 3.24$ (382). These lines fall within the absorption regions depicted in Fig. 1, and the first two lines fall within the luminescence regions described by Meidinger [17].

In the series $h\nu_{in} = (E_g - R''hc/4^2) - R''hc/n^2$ we have lines with $h\nu_1 = 2.326$ (533), $h\nu_2 = 3.07$ (405), $h\nu_3 = 3.26$ (331), etc. For other series with small values of $R''hc/n^2$ ($n = 5, 6, 7, \ldots$) we have lines some of which fall into the blue luminescence band, while the others group around the series limit with $h\nu_\infty = E_g$.

For the group of series $h\nu_{in} = (E_g - iR''hc) - R''hc/n^2$, where $i = 1$, $1 - (1/2)^2$, $1 - (1/3)^2$, $1 - (1/4)^2$, ..., the first lines $h\nu_{i1}$ fall into the infrared (IR) band, while all the others fall into the bands lying within the 440–560-nm interval. The limits of this group of series coincide with the maximum at roughly 2.4 eV (515 nm), which is clearly seen in Fig. 1. This absorption band corresponds to the luminescence band discovered by Kanzaki et al. [14] and Meidinger [17].

The entire series $(E_g - 2R''hc) - R''hc/n^2 = 1.39 - 0.994/n^2$, except for the first line ($h\nu_1 = 0.38$ eV) falls into the IR band. The line $h\nu_\infty = 1.39$ eV resides close to the maximum of this band (see Fig. 1).

The above series and lines correspond to luminescence bands caused by the presence of isoelectronic impurities, such as chlorine and some others. We described the spectra of AgBr in the same manner as we did for AgCl, assuming that $E_g = 3.0775$ eV (24823 cm^{-1}) and $R'hc = 0.4564$ eV (3681 cm^{-1}) [9]. We assume, as we did earlier, that light absorption is accompanied by the formation of hydrogen-like systems, for which $\mu \cong m_e^*$ and $R'' = 2R'$.

In the series $h\nu_{in} = E_g - R''hc/n^2$ with $i = 0$ we have lines with $h\nu_1 = 2.15$ (572), $h\nu_2 = 2.85$ (435), $h\nu_3 = 2.98$ (415), $h\nu_4 = 3.02$ (410), $h\nu_5 = 3.09$ (408), and $h\nu_6 = 3.0775$ (403), which fall into the bluish broad luminescence band [17, 19].

In the series $h\nu_n = (E_g - R''hc) - R''hc/n^2$ with $i = 1$, the lines [except for the first line with $h\nu_1 = 1.255$ (890)], $h\nu_2 = 1.94$ (638), $h\nu_3 = 2.07$ (590), $h\nu_4 = 2.11$ (585), $h\nu_5 = 2.13$ (580), and $h\nu_6 = 2.165$ (571) fall into the luminescence bands observed by Kozyreva and Meĭklyar [5] and Kirillov and Fomenko [9]. Notwithstanding the fact that Kanzaki and Sakuragi [23] studied AgBr : I crystals while Kozyreva [24] the purified AgBr crystal, the spectra of these crystals observed at 2 and 4 K are almost the same.

In the series $h\nu_n = (E_g - R''hc/2^2) - R''hc/n^2$ with $i = (1/2)^2$ we have lines with $h\nu_1 = 1.94$ (638), $h\nu_2 = 2.62$ (473), $h\nu_3 = 2.75$ (450), $h\nu_4 = 2.9$ (445), $h\nu_5 = 2.81$ (440), and $h\nu_\infty = 2.847$ (456). The line for $h\nu_1$ falls into the bands discussed by Meidinger [17], the line for $h\nu_2$ falls into the bands discussed by Kirillov and Fomenko [9] and Moser et al. [15], and the other lines fall into a weak broad band discussed by Ryzhanov [6]. We also obtained series with $i = (1/3)^2, \ldots$, $(1/6)^2, \ldots \ldots$, $1 - (1/2)^2, \ldots$, $1 - (1/5)^2, \ldots$ Here, a sizable fraction of the lines fall into the absorption and luminescence bands of AgBr crystals with metal-ion impurities (Na^+, Cu^+, and Li^+) or with isoelectronic impurities (I^- and Cl^-). The calculated lines that fall within the IR portion of the spectrum lie outside the spectral interval studied in experiments. As in the case with AgCl, irrespective of the type of impurities, the series of lines with $i = (1/2)^2$, $(1/3)^2$, $1 - (1/2)^2$, $1 - (1/4)^2$ fall into the bright luminescence bands discussed in Refs [17,

18, 23 – 25] if one allows for the temperature dependence of ε [18]. Edge emission is caused by recombination of an electron with a localized or trapped hole or by recombination of a mobile hole with a trapped electron. The discussed possibility of the formation of absorption and luminescence spectra through the use of the hydrogen-like impurity model reduces the distinction between the spectra of excitons and hydrogen-like impurities to the difference expressed by the values of R'' and the number i in equation (2). The injection of positive ions into AgHal crystals leads to a situation in which the excitons formed by radiation with $h\nu < E_g$ dissociate in the field of a positive impurity ion, which results in the formation of a hydrogen-like system consisting of an electron and a 'localized' positive ion. When the introduced isoelectronic impurities (in the form of I^- and CI^-, for instance) absorb radiation with $h\nu < E_g$, the result is also hydrogen-like systems, the only difference being that now there is no free hole.

Hence, the edge absorption and luminescence spectra induced by photons of various energies incorporate series of lines described by equations (3) given below, both for crystals with impurity centers and for pure crystals, when the radiation generated primarily by exciton annihilation is formed in such crystals. In this case R' is used in calculations.

We would also like to note that the analysis of equation (3) at $i = 4$ for AgHal crystals suggests that formation of hydrogen-like centers with $Z = 2$ is also possible, for which there is no first state and the lines for photons with $h\nu_2, \ldots, h\nu_\infty$ fall within the visible region of the spectrum. We believe it is most likely that such additional spectra will appear in microcrystalline layers (fine powders and photographic materials), in which exposure to actinic radiation leads to a relatively intense photochemical decomposition of the substances. Experience does not contradict this assumption, since the luminescence spectra of thin films and fine powders are more diffused than the spectra of single crystals. Notice that we have described the formation of a broad absorption band in the interval from 365 to 900 nm in finely crystalline and single-crystal AgBr and AgCl thin films, a band induced by light with $h\nu < E_g$ at room temperature. In the interval from 600 to 900 nm, light-absorption and photoeffect centers in AgHal crystals are silver subparticles, whose size depends on the intensity of light and exposure time.

At low temperatures, the band gap E_g in crystals has to be the threshold of the continuous optical-absorption spectrum. At the same time, in AgHal crystals the maxima in the photocurrent and photochemical (photographic) sensitivity as well as the edge luminescence lines can be observed when the photons have energies $h\nu$ smaller than the band gap E_g. The emergence of these maxima and lines can be explained if we assume that the result of absorption of light with $h\nu < E_g$ is the formation of Wannier – Mott excitons and 'localized' excitons [20, 21] with a binding energy that is twice that of the Wannier – Mott exciton ($R''hc = 2R'hc$). Since the exciton binding energy depends on the dielectric constant ε, the values of E_g, R', and ε for AgHal crystals become correlated. The values of E_g at room temperature for AgBr (3.05 eV), AgCl (3.25 eV), and AgI (3.02 eV) and at 4.2 K for the same crystals (3.077, 3.38, and 3.023 eV, respectively) are given in Refs [15, 20, 21]. The values of E_g at 293 K for these crystals were obtained from the positions of the photocurrent maxima, while the values at 4.2 K were refined via the luminescence spectrum lines, for which the photon energies $h\nu$ were smaller than E_g.

Above we listed our values of the binding energy of the Wannier – Mott excitons at 293 K (0.242 eV for AgBr, and 0.261 eV for AgCl) under the assumption that $m_e = m_h$, while the values of ε determined through experiments proved to be equal to 5.3 for AgBr and 5.2 for AgCl. Using the luminescence spectra referred to by Kozyreva and Meĭklyar [5], we found the values of $R'hc = 0.456$ eV for AgBr and 0.497 eV for AgCl at 4.2 K. The photoelectric data for AgBr, extrapolated from 293 K to 4.2 K, were used to find the value $R'hc = 0.455$ eV [4], with allowance for a change in the dielectric constant ε from 5.3 to 3.87 as the temperature was reduced.

At 4.2 K, we have $E_{g1}/E_{g2} = 3.387/3.077 = 1.1$, and $R'_1hc/R'_2hc = 0.497/0.457 = 1.09$. Allowing for the fact that $R'hc = \mu e^4/2\hbar^2\varepsilon^2$, where μ is the reduced exciton mass expressed in terms of the electron mass, we arrive at two corollaries:

(1) The value of μ does not vary with temperature. This result was achieved (see Refs [20, 21]) by comparing the energy separation of the photocurrent maxima at 293 K and the corresponding luminescence lines at 4.2 K.

(2) The product $E_g\varepsilon^2$ for AgBr and AgCl crystals assumes a certain value at given temperature and light frequency, since E_g depends (but weakly) on temperature while ε depends on the temperature and light frequency.

Using our data on E_g and ε, we have (at 293 K) $E_{g1}\varepsilon_1^2 = 3.05 \times (5.3)^2 = 85.2$ for AgBr and $E_{g2}\varepsilon_2^2 = 3.25 \times (5.1)^2 = 84.5$ for AgCl; at 4.2 K we have $E_g\varepsilon_1^2 = 3.077 \times (3.87)^2 = 46.2$ for AgBr. Lacking the corresponding, independently determined value of ε for AgCl, we assumed, on the grounds that the values of $E_g\varepsilon^2$ for AgBr and AgCl are the same at 293 K, that the values of ε are equal at 4.2 K, too. Then from the relationship $3.38\,\varepsilon_2^2 = 46.2$ we find that $\varepsilon_2 = 3.71$. This value is used below and, as we will see shortly, coincides with the value obtained from another relationship. Earlier, Moss [26] assumed that the optical band gap varies as $\bar{n}^{-4}$ or $E_g\bar{n}^4 = \text{const}$, with $\varepsilon = \bar{n}^2$, which holds for the long-wavelength segment of the absorption band. For 18 semiconductors and insulators, Moss fixed the average value of $E_g\varepsilon^2$ at roughly 77 eV, with a spread ranging from 66 to 170 eV. The reason for such a spread probably lies in the fact that Moss used values of $\bar{n}^2$ for radiation belonging to different portions of the spectrum and, possibly, at different temperatures, while the values of ε we have listed were obtained through measurements of light reflection at a frequency corresponding to the excitonic maximum. For different substances, the temperature coefficient of the dielectric constant, $\mathrm{d}\varepsilon/\mathrm{d}T$, may be either positive or negative. The temperature dependence of E_g was also not mentioned by Moss. An example of how these factors may be taken into account is the use of low-frequency values of the dielectric constant ε_0 for AgBr (13.1) and AgCl (12.3) at 293 K: $E_g\varepsilon_0^2 = 3.05 \times (13.1)^2 = 552$ for AgBr, and $3.25 \times (12.3)^2 = 492$ for AgCl. According to these data, the deviation from the average value is roughly 3%.

In AgHal crystals, as the layer thickness of the sample under investigation increases (starting from 10^{-5} cm or larger), maxima appear in the photocurrent and absorption spectrum, which are caused by light with an energy $h\nu < E_g$ (there are no such maxima in very thin films). In AgHal at 4.2 K, E_g lies within the 3.023 – 3.38-eV interval, and the absorption edge is in the longer-wavelength portion of the spectrum, with an energy $h\nu = E_g - R'hc$ or $h\nu = E_g - R'hc/n^2$ corresponding to this edge, i.e. the observed edge of

the broad optical-absorption band, corresponding to excitonic absorption, differ from E_g by $R'hc$ or by $R'hc/n^2$. For such crystals as germanium and diamond, for which ε is 16 and 5.7, respectively, the difference between E_g and $h\nu = E_g - R'hc$ is small: for germanium it is 0.0015 eV, and for diamond it is 0.075 eV. Bearing in mind that for germanium $E_g = 0.7$ eV and for diamond the value is 5.5 eV, we can assume that the optical absorption edge coincides with E_g, but for silver halides and similar crystals the difference is $0.08E_g$ at room temperature and up to $0.15E_g$ at 4.2 K. If the absorption edge in AgHal is formed by 'localized' excitons, the difference specified above doubles.

Going back to the ratio $R_1'hc/R_2'hc$ and allowing for the dependence of the exciton binding energy on ε and μ, we can write $(R_1'hc)\varepsilon_1^2/\mu_1 = (R_2'hc)\varepsilon_2^2/\mu_2 = 13.6$ eV on the grounds of the experimental data on these crystals.

Since $\mu_1 = \mu_2 = 0.5$ at all temperatures, then according to our experimental data at 293 K for AgBr we have $R'hc\varepsilon_1^2 = 0.242 \times (5.3)^2 = 6.75$ eV, and for AgCl we have $R'hc\varepsilon_2^2 = 0.261 \times (5.1)^2 = 6.8$ eV. At 4.2 K, for AgBr we have $R_1'hc\varepsilon_1^2 = 0.456 \times (3.87)^2 = 6.8$ eV. For AgCl, using the value $\varepsilon = 3.71$ obtained earlier, we find that $(R_2'hc)\varepsilon_2^2 = 0.497 \times (3.71)^2 = 6.8$ eV. In contrast to $E_g\varepsilon^2$, the product $(R'hc)\varepsilon^2$ is temperature independent. Hence we arrive at the natural conclusion that for light-sensitive crystals in the relationships $E_{g1}\varepsilon_1^2 = E_{g2}\varepsilon_2^2$ and $R_1'hc\varepsilon_1^2 = R_2'hc\varepsilon_2^2$ the values of ε for one crystal can be used in determining ε for another crystal.

If we apply the above relationship to AgI crystals, the result is somewhat different. According to our experimental data, the reflection from thin polycrystalline layers of AgI at 293 K is fractions of a percentage point greater than the reflection from AgBr in the vicinity of the first excitonic maximum ($\lambda = 420$ nm). Using the relationship $E_g\varepsilon^2 = 85.2$, we find that $\varepsilon = 5.35$ in accordance with the experimental data, and $R'hc = 13.6/\varepsilon^2 = 0.23$ eV. In addition, according to Ryzhanov's calculations [1], $R'hc$ for AgHal is half the energy separation of the peak in the photoeffect, corresponding to the 'band-to-band' transition, and the first excitonic peak corresponding to $h\nu = E_g - R'hc$.

For the first peak we have $h\nu = 3.39$ eV ($\lambda = 365$ nm), and for the second, 2.95 eV (420 nm). According to these data, the value of $R'hc$ for AgI is 0.222 eV, which was determined from the luminescence lines [20]. Since the product $R'hc\varepsilon^2 = 6.8$ eV is temperature independent, ε for AgI changes very little as the temperature goes lower. The relationships we derived for AgHal imply that

$$\frac{E_{g1}}{E_{g2}} = \frac{R_1'hc}{R_2'hc} = \frac{\varepsilon_2^2\mu_2}{\varepsilon_1^2\mu_1}.$$

Allowing for the above, we can write an equation that determines the absorption and luminescence lines caused by Wannier–Mott excitons in a form that will make it possible to pass from the excitonic spectrum of AgBr to the excitonic spectrum of AgCl and back, including series for which the limit is one of the levels of a Wannier–Mott exciton or the level of a 'localized' exciton:

$$h\nu_{in} = \left[(E_{g2} - iR_2'hc) - \frac{R_2'hc}{n^2}\right]\frac{\varepsilon_2^2}{\varepsilon_1^2} \quad \text{for} \quad \text{AgBr}, \qquad (3)$$

$$h\nu_{in} = \left[(E_{g1} - iR_1'hc) - \frac{R_1'hc}{n^2}\right]\frac{\varepsilon_1^2}{\varepsilon_2^2} \quad \text{for} \quad \text{AgCl}.$$

For the lines of the corresponding series to coincide, the brightness of the appropriate lines must be sufficient for observing these lines. The same must hold for crystals containing excited impurities ('localized' excitons) for which, consequently, the above relationships are valid.

The above discussion is corroborated by the following experimental data on luminescence, photocurrent, and photolysis of silver halides.

Our calculations [20] for AgBr resulted in the following series of lines (cm^{-1}) with $i = 8/9$:

$$\nu_{in} = \left(\frac{E_g}{hc} - \frac{8}{9}R'\right) - \frac{R'}{n^2},$$

where some of the lines were observed earlier by Kozyreva and Meĭklyar [5]; we also calculated the same series for AgCl. Five lines out of the eight calculated for each series were examined in experiments. The results of calculations for AgBr coincided perfectly with the experimental data, while for AgCl the discrepancy was 1–3 cm^{-1} for four lines, and 13 cm^{-1} for the fifth line. If the wave numbers of the series in question for AgBr are multiplied by $\varepsilon_1^2/\varepsilon_2^2 \cong 1.1$, we arrive at the corresponding series for AgCl, whose lines are given in Ref. [5] (Table 7).

This implies that calculations by the equations of the form (3) lead to meaningful results for any of the series referred to in our papers [20, 27].

Kanzaki et al. [14] listed the characteristics of the luminescence band for an unrefined AgBr crystal at 4.2 K. The short-wavelength edge of the band is 500 nm (2.47 eV), the long-wavelength edge is 595 nm (2.08 eV), and the maximum is at 536 nm (2.31 eV). Kozyreva [24] listed the data on the luminescence band that emerges in AgCl at 2 K. The short-wavelength edge of this band is 444.4 nm (2.78 eV), the long-wavelength edge is 550 nm (2.25 eV), and the maximum is at 495 nm (2.5 eV). AgCl has such characteristics of its luminescence band if we multiply the above data on the band for AgBr by the ratio $\varepsilon_1^2/\varepsilon_2^2 = 1.1$. Indeed, it follows that $2.47 \times 1.1 = 2.72$; $2.08 \times 1.1 = 2.29$, and $2.31 \times 1.1 = 2.54$, which are almost the corresponding values for AgCl. Here we must bear in mind that the data on the luminescence bands were taken from small diagrams; more than that, the temperature of AgBr differed from the temperature of AgCl. We assume that to each line belonging to the band for AgBr there corresponds a line in the band for AgCl, the latter can be obtained from the former through multiplication by $\varepsilon_1^2/\varepsilon_2^2$. Thus, this is one more argument in

Table 7.

n	2	3	4	5	6	7	8	∞
ν_n, cm^{-1}, AgBr	20631	21142	21321	21404	21449	21476	21494	21551
ν_n, cm^{-1}, AgCl (expt.)	22714	22272	Undetected	Undetected	23602	23634	23653	23719
ν_n, cm^{-1}, AgCl (theory)	22708	23271	23468	23559	23608	23638	23658	23721

favor of our idea that the formation of these luminescence bands is caused by hydrogen-like systems.

Thus we see that excitons are described by hydrogen-like formulas, from levels corresponding to large values of n to the level corresponding to $n = 2$. The characteristic radius of an exciton in AgBr for $n = 2$ is $r_2 = (\varepsilon_1/\mu_1)n^2 r_B = 22$ Å $\cong 7d$ (here r_B is the Bohr radius of the hydrogen atom in the ground state, and d is the lattice constant). Hence, for such an exciton radius no substantial deviations from laws governing hydrogen-like systems are observed.

If the position of the short-wavelength photocurrent maxima on the corresponding spectral characteristics for AgBr is compared to that for AgCl (see Figs 51 and 55 of monograph [4]), corresponding to 430 and 393 nm in wavelength (or 2.87 and 3.14 eV, respectively), we find that $3.14/2.87 = \varepsilon_1^2/\varepsilon_2^2 = 1.1$. If the position of the longer-wavelength photocurrent maxima on the corresponding spectral characteristics for AgBr is compared to that for AgCl, with both sets measured by Kirillov and Fomenko (see Figs 53 and 57 in Ref. [4]), we have $3.05/2.7 = 1.13$.

Comparison of the positions of the maxima on the spectral characteristics of the photosensitivity inherent in finely crystalline photolayers of AgBr and AgCl, obtained by Breĭdo and Gorokhovskiĭ (see Fig. 72 of Ref. [4]) yields $3.5/3.1 = \varepsilon_1^2/\varepsilon_2^2 = 1.14$.

According to a report done by Silukova [28], studies of phenomena based on electronic excitations in gold bromide and chloride revealed that the peak in luminescence in crystalline films of these substances corresponds to photon energies of 2.57 and 2.89 eV, respectively. The corresponding band gaps E_g are 2.7 and ~ 3 eV. The ratio of these values amounts to 1.1, as for the AgHal crystals described above. The ratio of band gaps in AuHal was found from the diagrams of the above paper.

Thallium halides (Figs 2 and 3) are photochemically active substances for light with a photon energy higher than that for silver halides, whose long-wavelength absorption edge falls within the visible region of the spectrum.

Earlier we found that

$$\frac{E_{g2}}{E_{g1}} = \frac{R_2' hc}{R_1' hc} = \frac{\varepsilon_1^2}{\varepsilon_2^2} = 1.1\,,$$

where the subscripts 1 and 2 refer to AgBr and AgCl, respectively, E_g is the band gap, $R'hc$ is the binding energy of the hydrogen-like system consisting of an electron and a hole in the unexcited state (a Wannier – Mott exciton or a 'localized' exciton — excited impurities or defects in the AgBr and AgCl crystals), and ε is the dynamic dielectric constant of the crystal for values of $h\nu_i$ from the interval $(E_g, E_g - R'hc)$.

What we have just said refers not only to lines but also to absorption and luminescence bands excited in these crystals. Each line in these bands has a line corresponding to it in the absorption or luminescence band of the other crystal, and the ratio of the photon energies corresponding to lines in these bands is equal to the ratio of the squares of the respective dielectric constants: $h\nu_1/h\nu_2 = \varepsilon_2^2/\varepsilon_1^2$. The positions of the maxima of photographic sensitivity as well as the long- and short-wavelength maxima of photocurrent on their spectral characteristics at the same temperature and for the same structure of the crystalline layers can also be found through the ratio $\varepsilon_1^2/\varepsilon_2^2 = 1.1$.

The above regularities follow from the existence of systems possessing hydrogen-like properties, systems whose formation and dissociation bring about the photochemical processes that take place in the light-sensitive crystals.

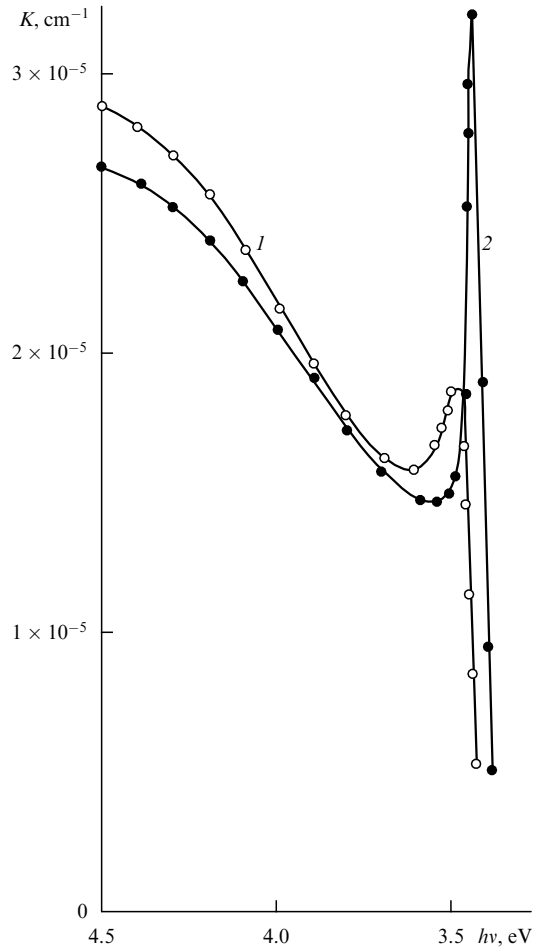

Figure 2. Self-absorption edge of TlCl. The layer was grown on a single crystal of KCl at room temperature. Curve *1* corresponds to a temperature of 26 °C, and curve *2* to a temperature of −185 °C [29].

This is also true of thallium halides.

When we speak of the similarity of the spectral characteristics of optical absorption in TlHal to those in AgHal, we mean that, according to Tutihasi [29] and Figs 2 and 3, there are sharp peaks at the absorption edge of each substance at 88 K. In TlCl this peak corresponds to 3.44 eV, and in TlBr, 3.1 eV. The ratio of these values is 1.1, as for silver halides, and it does not vary with temperature. We can assume (just as we did with AgHal) that these peaks correspond to the formation energy of ground-state excitons with $n = 1$, i.e. $3.44 = E_{g1} - E_{g1(1)}$ and $3.1 = E_{g2} - E_{g1(2)}$.

Determining the approximate value of the band gap in TlHal at 88 K from the above characteristics and using the Moss criterion [26] in the same way as was done for AgHal, from the spectral characteristics of the photoelectric sensitivity (at the $\lambda_{1/2}$-point, which is the light wavelength at which the photosensitivity is half the maximum value) we find that $E_g = 3.76$ for TlCl and $E_g = 3.385$ eV for TlBr. Then at 88 K for TlCl the value of the binding energy of the exciton in the ground state, $R_2' hc = E_{g2} - E_{g1(2)}$, is $3.76 - 3.44 = 0.32$ eV, while for TlBr $R_1' hc = 3.385 - 3.1 = 0.285$ eV. In this case, too, the ratio $E_{g2}/E_{g1} = R_2' hc/R_1' hc = 1.1$, as it is for AgHal. In all these examples the values of the quantities were determined from the graphs in the cited works.

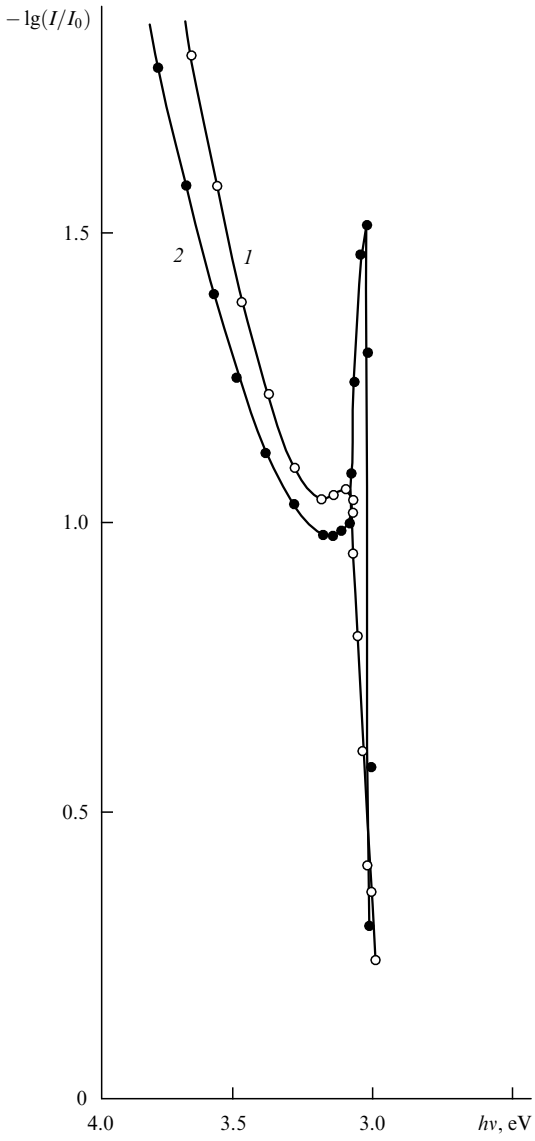

Figure 3. Self-absorption edge of TlBr. The layer was grown on a quartz substrate at room temperature. Curve *1* corresponds to room temperature, and curve *2* to the temperature of liquid air [29].

On the basis of the results just discussed we assumed that this ratio holds for the squares of the dielectric constants of TlBr and TlCl. Then for these compounds the product $E_g\varepsilon^2$ is the same for equal room temperatures, i.e. at 293 K we have $E_g\varepsilon^2 = 85.2$. The temperature coefficient of the dielectric constant for TlHal is approximately 3.2 times smaller than that for AgHal. Using plots in Figs 2 and 3 to determine the values of E_g for TlBr (3.31 eV) and for TlCl (3.72 eV), we find that $\varepsilon_1^2 = 25.8$ and $\varepsilon_2^2 = 23.1$. From the positions of the peaks in absorption we determine the values of $R'hc = E_g - E_{g1}$: for TlBr we have $R'hc = 0.25$ eV, and for TlCl, 0.285 eV. In contrast to $E_g\varepsilon^2$, the product $R'hc\varepsilon^2$ is temperature independent and amounts to 6.8 eV for the same reduced mass $\mu = 0.5m_e^*$. Using the above values of $R'hc$ and ε^2 for TlBr and TlCl, we get 6.45 and 6.58 eV, respectively. [1] Naturally, more accurate values of E and $R'hc$ for these substances can be found from the fine structure of the absorption or luminescence spectrum.

Comparison of the spectral characteristics of optical absorption for TlHal and AgHal shows that the maxima at the absorption edge for TlHal are shifted to the ultraviolet (UV) region of the spectrum in relation to similar peaks for AgHal, and that E_g for TlHal becomes larger than the value for AgHal. We believe that these changes are due primarily to the difference in the properties of the Tl^+ ion and the Ag^+ ion in the crystal lattices that these ions form with the halide ions. Below we will show how these changes in properties can be taken into account.

These results corroborate the fact that the absorption and luminescence spectra of the light-sensitive AgHal and TlHal crystals are caused by hydrogen-like systems that form in these crystals and that the regularities discussed here describe the photoelectric and photochemical processes leading to the formation of latent photographic images. The extensive activity in the fields of photography and cinema selected, from all these substances, AgBr with an admixture of AgI primarily because of the band gap E_g, which is the smallest in this group of substances, and the values of the dielectric constant ε, which make it possible for the hydrogen-like systems that form in this substance to have their energy levels in the visible region of the spectrum, corresponding to such sources of light as the Sun and other highly heated (incandescent) bodies.

The other significant factors are the capacity of the finest metal particles to coagulate and the topochemical nature of the photolysis of the halides in question [30].

Meticulous investigations of excitonic states in lead halides have been conducted at the Physics Institute of the Estonian Academy of Sciences (Tartu). When the light absorption and luminescence spectra of lead halides [31 – 35] are compared with the respective bands of silver and thallium halides in Figs 2 and 3, a certain resemblance can be seen if we take into account the relative shift of the bands' maxima and their low-frequency edges.

Élmas and Kink [31] presented the absorption spectra of $PbCl_2$ and $PbBr_2$ at 295 and 100 K. Comparing the peaks on the spectral characteristics of these substances, we see that the corresponding photon-energy ratios are 4.5/3.7 (at 295 K) and 4.6/3.8 (at 100 K); in both case this ratio is equal to 1.2. At the energies of the band-to-band transitions for $PbCl_2$ (5.0 eV) and $PbBr_2$ (4.2 eV) given by Élmas and Kink [31], the ratio of interest is equal to 1.19. These ratios also change very little for the maxima of the absorption bands in $PbCl_2$ and $PbBr_2$ at 4.2 K [32], with the corresponding photon energies being 4.69 and 3.99 eV ($4.69/3.99 = 1.18$).

According to Élmas and Kink's data [31], the ratio of the band-to-band transition energies for $PbCl_2$ and $PbBr_2$, obtained from the 'steps' in the luminescence spectra at 4.2 K, is equal to $5.38/4.38 = 1.2$.

Lidja et al. [34] presented the reflectance spectrum of $PbBr_2$ (in the interval from 3.9 to 4.6 eV) and $PbCl_2$ (in the interval from 4.6 to 5.0 eV). Lidja et al. [32, 36] extended this spectrum into the UV region to an energy of 5.75 eV. We used these spectra and the Fresnel formula with allowance made for the fact that $\bar{n} = \sqrt{\varepsilon}$ and calculated the values of ε for photons with energies corresponded to the band gap in $PbCl_2$ ($E_g = 5.38$ eV) and $PbBr_2$ (4.38 eV); the respective values were $\varepsilon_2 = 4.3$ and $\varepsilon_1 = 4.7$. The ratio $\varepsilon_1^2/\varepsilon_2^2$ was found to be equal to $(4.7)^2/(4.3)^2 \approx 1.2$. The products of band-to-band transition energies (5.0 eV for $PbCl_2$ and 4.2 eV for $PbBr_2$) by

[1] Allowing for the fact that the temperature coefficient of the dielectric constant, $\varepsilon^{-1}\,d\varepsilon/dT$, is equal to 2.8×10^{-4} K^{-1}, we arrive at the same values of $(R'hc)\varepsilon^2$ at $T = 88$ K.

the respective values of ε_1^2 and $\varepsilon_2^2 1$ are almost the same: $E_g\varepsilon^2 = 5.0 \times (4.3)^2 \cong 4.2 \times (4.7)^2 \approx 92.5$. For the other band-to-band transition (5.38 eV for $PbCl_2$ and 4.38 eV for $PbBr_2$), the products $E_g\varepsilon^2$ differ by 2.5%.

The above regularity is observed when one compares the luminescence spectra of nonactivated PbHal crystals obtained by Plekhanov and Lidja [35]; the researchers refer these spectra to luminescence caused by cation excitons. Comparison of luminescence spectra shows that the ratio of the photon energies corresponding to the maxima of these bands (4.8 and 4.5 eV for $PbCl_2$) to the photon energies corresponding to the maxima of the respective bands in $PbBr_2$ (4.1 and 3.85 eV) amounts to 1.18. For polarization spectra of $PbCl_2$ and $PbBr_2$, the ratio of maxima with $h\nu = 2.15$ and 1.8 eV is also equal to 1.18. The current comparison of the experimental data with allowance for the structure of the crystalline layers makes it possible to extend the regularities observed for AgHal to $PbHal_2$.

Note that Kink et al. [37] and Belous et al. [38] also describe the phenomena related to excited states in AgHal, the behavior of 'localized' excitons of different origin, and the interaction of these excitons with the surroundings in different crystals under various conditions and cite a large number of papers used in their investigation.

If the irradiation of crystals of simple metal compounds with bromine by photons of energies $h\nu \leqslant E_g$ causes a photochemical effect or luminescence, the irradiation of compounds consisting of the same metals and chlorine with photons of energies $h\nu \leqslant E_{g1}$ causes the same effect when the photon energy ratio $h\nu_1/h\nu = \varepsilon^2/\varepsilon_1^2$ is 1.1.

For AgHal and TlHal, the ratio $\varepsilon^2/\varepsilon_1^2 = 1.1$ is temperature independent. A particular case when this relationship holds is $E_{g1}/E_g = \varepsilon^2/\varepsilon_1^2$.

On the basis of the above experimental data for AgHal and TlHal at room temperature, we have $E_g\varepsilon^2 = E_{g1}\varepsilon_1^2 = \text{const} = 85.2$.

Below instead of E_g we use the values of the photon energies corresponding to the optical absorption edge (E_{opt}) at the same temperature. This quantity differs from E_g by $R'hc/n^2$. Assuming that this relation is also true for other simple ionic crystals, we use it to determine ε^2 of alkali halide crystals. According to Fig. 23 of Ref. [4], which gives the classical results of measurements of absorption in the U- and F-bands at 293 K, we see that the value $E_{opt} = 6.85$ eV corresponds to the edge of the absorption band for the KCl crystal; for KBr this value is 6.35 eV, and for NaCl, 7.4 eV.

Fixing $E_g\varepsilon^2$ at 85.2, we find the values of ε^2 for KCl (12.4), KBr (13.4), and NaCl (11.5). We will now employ these values to find the binding energy $R''hc$ of a 'localized' exciton for which the reduced mass obeys the formula $\mu/m_e = 1$. The value of $R''hc$ can be found from the relationship $R''hc\varepsilon^2 = 13.6$ eV, which holds true at all temperatures. Using the above values of ε^2, which are temperature dependent, we find that at 293 K $R''hc = 1.1$ eV for KCl, 1.0 eV for KBr, and 1.2 eV for NaCl.

The values of $R''hc$ for KCl and KBr coincide with the experimentally established difference between the values of the optical band gap E_{opt} and the first maximum at the absorption edge (these values have been found by Fowler [39]). The following photon energies correspond to the experimentally determined maxima of the U-band in the given crystals: 5.76 eV (214 nm) for KCl, 5.42 eV (228 nm) for KBr, and 6.42 eV (192 nm) for NaCl. The width of the U-band is 1.1 eV. Finally, the position of the maxima of the U-band can be calculated by the formula $h\nu_n = E_{opt} - R''hc/n^2$.

The value of $h\nu_1$ in KCl for the level with $n = 1$ is $6.85 - 1.1 = 5.75$ eV (the discrepancy with the experimental value is 0.01 eV); for KBr we have $h\nu_1 = 6.35 - 1.0 = 5.35$ eV (the discrepancy is 0.07 eV), and for NaCl we have $h\nu_1 = 7.4 - 1.2 = 6.2$ eV (the discrepancy is 0.22 eV). For these salts all the calculated values of $h\nu_2$, $h\nu_3$, ..., $h\nu_n$ fall into the experimental interval between a maximum of the U-band and the optical absorption edge E_{opt}.

The following photon energies correspond to the maxima of the F-bands in the three salts: 1.96 eV (630 nm) for KCl, 2.19 eV (563 nm) for KBr, and 2.65 eV (465.9 nm) for NaCl. The photon energy ratio for KCl and KBr is $2.19/1.96 = 1.1$. For these crystals, one finds

$$\frac{E_{opt,1}}{E_{opt}} = \frac{h\nu_{U1}}{h\nu_U} = \frac{h\nu_{F1}}{h\nu_F} = \frac{\varepsilon^2}{\varepsilon_1^2} = 1.1$$

at all temperatures. What we have just said is true of other bands observed in alkali halide crystals. According to Saint-James [40], in KBr and KCl the position ratios for the maxima of such absorption bands as R_1^-, R_2^-, and M_1^- (which are ascribed to colloidal particles) are 735/658, 790/727, 892/820, and 920/825 (the wavelengths are in nanometers). All these ratios are roughly equal to 1.1. For such bands and the F-band such a position ratio of their maxima is observed in RbBr and RbCl crystals. The position ratios for the maxima of the V-bands (V_1, V_2, V_3, and V_4) in KBr and KCl are also 1.1 with a deviation amounting to 2–4%.

For KBr and KCl crystals, the six absorption bands in the spectral region between the F- and M-bands described by Yagi [41] and denoted R_α, R_β, R_γ, R_δ, R_ε, and R_ξ are positioned in such a way that the maxima ratios are $847/782 = 795/738 = 780/700 = 741/671 = 704/635 = 669/608 = 1.1$. The position of the maxima in the H-bands obeys the same rule. The above suggests that from the energy viewpoint these centers possess the properties of hydrogen-like systems whose radius is larger than the lattice constant of the crystals ($r > d$) within which these systems reside.

Taking all this into account, we can say that the absorption of light by colloidal particles forming an M-band occurs at the metal–insulator interface. When the crystal is illuminated with light belonging to the M-band, the crystal exhibits relatively low photoconductivity whose spectral characteristic is close to that of photoelectric emission from the surface of the metal [40]. This phenomenon was observed for silver particles in AgHal and was described in Refs [42, 43] as photoelectric emission from colloidal silver particles into the surrounding insulator. The ratio of the band maxima for the photocurrent from the colloidal silver particles in AgCl and AgBr is also $\varepsilon^2/\varepsilon_1^2 = 1.1$.

For crystals that form as a result of a combination of Li, Na, K, Rb, or Ag and bromine or chlorine, the ratio of the squares of their lattice constants is 1.1 as well. For instance, for the pairs LiBr/LiCl, RbBr/RbCl, and AgBr/AgCl this ratio is, respectively, $d^2/d_1^2 = 2.74^2/2.56^2 = 3.43^2/3.27^2 = 2.88^2/2.77^2 = 1.1$, with deviations from the average value in the 1–2% range (the values of d are given by Fowler [39] in angstroms). Then one obtains $h\nu_1/h\nu = d^2/d_1^2 = 1.1$ and $E_{g1}/E_g = d^2/d_1^2 = 1.1$. Or $h\nu d^2 = h\nu_1 d_1^2 = \text{const}$ and $E_g d^2 = E_{g1} d_1^2 = \text{const}$. The latter expressions coincide with Mauleveau's formula $\nu d^2 = \text{const}$ [44], which was originally written for the F-band of alkali-metal chlorides.

According to the data listed above, the formula $vd^2 =$ const holds good for any lines in absorption, photoconductivity or luminescence spectra of the given crystals, differing only in the value of the constant. For instance, the above data imply that for the maxima of the U-band in KBr and KCl, if we take hv (in electron-volts) instead of v, we get $hvd^2 = 57.8$ eV Å^2, with the deviation from this magnitude being in the 1–1.5% range. For the maxima of the F-band in the same crystals, $hvd^2 = 22.5$ eV Å^2 (on the average), with the deviation from the average being within 4.5% for NaCl [17]. For the maxima of the R_1-band in KCl and KBr (658 and 735 nm [45]), we have $hvd^2 = 18.7$ eV Å^2 (on the average), with the deviation from the average being 0.5%. There are numerous other examples of this type. The ratio of the constants in these examples for $hv \leqslant E_{opt}$ become smaller and smaller (compared to unity) as photons of lower energies are involved.

We must point out the regularity that links the lattice constant d of alkali halide crystals to the radii of the ions forming the crystal lattice. For the AgBr crystal, $d = 2.88$ Å; for the AgCl crystal, the value is 2.77 Å; for RbBr it is 3.43 Å, and for RbCl it is 3.27 Å. The ionic radii of Br^-, Cl^-, and Ag^+ are, respectively, 1.95, 1.81, and 1.13 Å [46].

For AgBr and AgCl, the ratio of the squares of the sums of ionic radii r is equal to the ratio of the squares of the lattice constants, so that one obtains: $(1.13 + 1.95)^2/(1.13 + 1.81)^2 = 2.88^2/2.77^2 = 1.1$. The ionic radius of Rb^+ is 1.49 Å, and the ratio of the squares of the ionic radii for RbBr and RbCl measures $(1.49 + 1.95)^2/(1.49 + 1.81)^2 = 1.09$. For NaBr and NaCl, this ratio is $(0.98 + 1.95)^2/(0.98 + 1.81)^2 = 1.1$. The ionic radius of Li^+ is 0.68 Å, and the ratio of the squares of the ionic radii for LiBr and LiCl comes to $(0.68 + 1.95)^2/(0.68 + 1.81)^2 = 1.1$.

Hence, the expression in question can be written as

$$\frac{h\nu_1}{h\nu} = \frac{\varepsilon^2}{\varepsilon_1^2} = \frac{d^2}{d_1^2} = \frac{(r_{Me^+} + r_{Br^-})^2}{(r_{Me^+} + r_{Cl^-})^2}$$

or, for simple compounds of metals and halogens, as

$$\frac{\varepsilon}{\varepsilon_1} = \frac{r_{Me^+} + r_{Br^-}}{r_{Me^+} + r_{Cl^-}} = \frac{d}{d_1}\,.$$

Clearly, for alkali halide crystals, as for AgHal, the positions of the luminescence lines and the maxima of photocurrent and photochemical sensitivity are described by the above ratios for ε, r, and d, provided that the crystals have the same temperatures. Naturally, these ratios can be used to find quantities referring to one crystal when the quantities characterizing other crystals are known.

Notice that when the photons have energies that exceed the band gap, $E_g < h\nu < 2E_g$, the regularities describing the behavior of photoelectrons in the band-to-band transitions are different. The temperature dependence of light absorption, photocurrent, and photosensitivity of silver–halide-based substances is almost proportional to the absolute temperature [47, 48].

3. Temperature dependence of the light sensitivity of unsensitized photographic materials and of photographic materials with heavy-metal compounds as impurities

In this section we generalize the results of investigations (carried out over a number of years) of the temperature dependence of silver halide photographic materials at the moment of exposure of the photosensitive layers and the effect of metal compounds on the light-sensitive properties of the photographic materials. The metal compounds were introduced into the photographic emulsions at the stage when the emulsions were ready to be poured onto different substrates (glass, porcelain, etc.). These materials were also heated for a short time ($\approx$ 5 min) to different temperatures at the moment of exposure.

The main experimental work was done using very fine-grained silver–iodine bromide photographic plates with a layer thickness of 10–12 μm and substrateless layers 25, 50, and 75-μm thick, not sensitized with optical dyes. The average diameter of the microcrystals was 30 nm. The AgBr content in the layer was roughly 75%, and the AgI content, about 1%. The initial photographic materials had the following sensitometric characteristics: $S_{0.85} = 10^{-2}$ All-Union State Standard (abbreviated GOST in Russian) units, $\gamma > 5$, $D_0 = 0.01$, and $D_{max} > 3$; the resolving power measured by holographic resolution meters was found to be about 2000 mm^{-1}.

The source of monochromatic radiation was the monochromator of an SR-4A spectrophotometer whose entrance slit was illuminated with the light from a hydrogen lamp (in the 200–350-nm spectral range) or an incandescent lamp (in the 350–1100-nm range).

The photographic material under investigation with the sample holder was placed in the path of the light beam emerging from the monochromator window. The light intensity was maintained constant in all the experiments.

To expose the emulsion layer at an elevated temperature, a device was used that consisted of a duralumin chamber with a copper plate 1-cm thick attached to one of its side. In order to heat the chamber, a preheated liquid (water, oil or glycerin, depending on the temperature to which the chamber was to be heated) was poured into it. The plate with the photographic material was pressed against the copper plate by steel springs. When the temperature of the photographic material reached the required one (the temperature was measured by a thermocouple), the sample was exposed to the monochromatic light. The exposure was done at the following temperatures: 20 °C (room temperature), 90 °C and 150 °C in the 250–500-nm range. The exposed samples were then developed for 3 min in a Phenidone–hydroquinone developer, with the optical densities measured by a DP-1 densitometer.

Table 8 lists the values of the optical density of the developed image for an emulsion layer of the laboratory-standard emulsion exposed at room temperature (the reference sample) and for emulsion layers heated, at the moment

Table 8. Temperature dependence of the optical density of the developed emulsion layer at the moment of exposure for different wavelengths of the light illuminating the samples.

Wavelength, nm	Optical density D			
	Temperature of exposed layer, °C			D_{150}/D_{20}
	20	90	150	
350	0.10	0.22	0.73	7.3
375	0.30	0.58	2.4	8
400	0.50	0.97	2.5	5
425	0.46	0.97	3.8	8.5
450	0.33	0.60	2.4	7.5
475	0.07	0.18	0.70	10
500	0.02	0.04	0.07	3.5

of exposure, to 90 °C and to 150 °C, with λ in the range 350 – 500 nm. We see that raising the temperature of the emulsion layer at the moment of exposure leads to a substantial increase in the optical density of the developed image.

Table 9 lists the optical densities of the developed image for substrateless emulsion layers 15-, 25-, and 75-μm thick that were exposed to light with $\lambda = 302$ nm at the same temperatures. We see that for these layers, too, the rise in the layer temperature at the moment of exposure from room temperature to 150 °C increases the optical density of the developed image in proportion to the increase of the absolute temperature.

Table 9. Temperature dependence of the optical density of developed substrateless emulsion layers (with $\lambda = 302$ nm).

Thickness d of emulsion layer, μm	Optical density D		
	Temperature of exposed layer, °C		
	20	90	150
15	0.58	0.71	0.84
25	0.72	0.88	1.01
75	0.94	1.16	1.35

To establish the effect of short-duration heating on the increase of the blackening density of emulsion layers (the same as in Table 8), the layers were maintained at a temperature of 150 °C in the same conditions as during exposure (for 5 min, the time during which the layer is heated and then exposed to light), cooled, exposed to monochromatic light, and developed. Table 10 lists the blackening density for the reference layers and the layers heated for 5 min at 150 °C and the then exposed to light at room temperature.

Table 10. Optical density of developed emulsion layers exposed at room temperature in the ordinary way and after preheating for 5 min.

Wavelength, nm	Optical density D	
	Reference sample	Exposure after heating and cooling
350	0.10	0.12
375	0.30	0.37
400	0.50	0.54
425	0.46	0.57
450	0.33	0.39
475	0.07	0.13
500	0.02	0.03

Comparison of the data in Tables 8 – 10 shows that when the photolayers are exposed to light in the heated state, the optical density is higher than it is in the case when the layers are exposed at room temperature after they are heated for the same time and cooled.

The above experimental results imply that the temperature dependence of the photosensitivity of unsensitized photographic materials for photons with energies $E_g < h\nu < 2E_g$ ($E_g = 3.05$ eV is the band gap for the AgBr crystal at room temperature) differs from that for photons with energies $h\nu < E_g$ [49 – 53].

Earlier we found (see Refs [54, 55]) that the temperature dependence of the photosensitivity of photographic layers not sensitized with optical dyes for photons with energies lower than the energy corresponding to the first (long-wavelength) excitonic maximum at the self-absorption edge ($h\nu < h\nu_0 = E_g - R'hc$, where $R'hc$ is the exciton binding energy in the state with $n = 1$) is described by the formula

$$\log S_\nu = \log S_0 \exp\left(-\sigma \frac{h\nu_0 - h\nu}{kT}\right),$$

where S_ν is the photosensitivity of the photographic layer for photons with $h\nu < h\nu_0$, S_0 is the same quantity for photons with an energy $h\nu_0$ (constant at a given temperature), T is the absolute temperature, k is the Boltzmann constant, and σ is a parameter characterizing the interaction between excitons and the thermal field of the crystal (phonons). The value of the photosensitivity S of a photographic layer was determined by the optical density D for constant exposure.

This regularity is a frequency – temperature characteristic for unsensitized photosensitive materials in a frequency range corresponding to an absorption edge caused by the formation of excitons in microcrystals during light absorption in the process of exciton – phonon interaction. It is corroborated by the experimental data [54 – 56] obtained at a fixed temperature.

The rise in the optical density, caused by the elevation of temperature from 293 to 393 K ($\lambda = 440$ nm), is characterized by the ratio $D_{393}/D_{293} = 0.36/0.19 = 1.9$. If we assume that the frequency – temperature characteristic for D, as well as for the absorption coefficient K, can be described by the Uhrbach rule [57] written for the absorption band caused by the formation of excitons and the exciton – phonon interaction, then one has

$$Kd = D = D' \exp\left(-\sigma \frac{h\nu_0 - h\nu}{kT}\right),$$

where D' is the optical density of the photolayer that absorbs photons with an energy $h\nu_0$ (the absorption edge), and d is the layer thickness, and for a rise in temperature from $T_1 = 293$ K to $T_2 = 393$ K with $-\sigma(h\nu_0 - h\nu) = 0.07 \times 0.22$ eV we obtain

$$\frac{\exp\left[-\sigma(h\nu_0 - h\nu)/kT_1\right]}{\exp\left[-\sigma(h\nu_0 - h\nu)/kT_2\right]} = 1.34\,.$$

This implies that the variation of D' for the given points 293 and 393 K is 0.15 and 0.21, respectively.

The value of the exciton – phonon coupling constant, $\sigma = 0.07$, obtained from the data of Refs [54, 55], is almost equal to the value $\sigma \sim 0.06$ calculated from our experimental data taken for the photosensitivity and photocurrent from Ref. [55]. More than that, for the coefficients of light absorption by mercury halides Deb [58] found the values of σ at 77 and 300 K being in the 0.02 – 0.06 range.

According to our earlier experimental data (see Refs [59, 60]) for light with $\lambda = 475$, 450, and 425 nm ($h\nu < E_g$), the ratio of the optical densities obtained under the same conditions of lighting and developing amounted, for exposures at 423 and 363 K, to 3.9, 4.0, and 3.9, respectively. For light with $\lambda = 400$ nm ($h\nu = E_g$), the ratio amounted to 2.6. The density ratio at 423 and 293 K for the above wavelengths amounted to 10, 7.5, and 8.5. In all cases, the fog density varied only slightly [59].

The elevation of temperature at the moment of exposure does not exclude the possibility of a rise in the integral sensitivity of photographic materials sensitized with optical dyes. For instance, the integral photosensitivity ($S_{0.85}$) of a film with panchromatic sensitization with a cyanine dye was

increased by a factor of 2.6 when the film was heated from 20 to 80 °C, but the fog density increased substantially in the process [59, 60].

Notice that there is another reason why the sensitivity of photographic materials increases when the temperature is increased immediately before exposure (this property is apparent primarily in highly sensitive photographic materials). The thing is that the latent-image centers consist of numerous closely packed silver atoms. In low-sensitivity photographic materials, the limiting factor is the decomposition of silver halides, which ensures the emergence of these atoms, while in highly sensitive photoemulsions such atoms have already been created at the crystal surfaces as a result of thermal decomposition of silver halides in the course of preparation of the photoemulsion. According to Galashin and Fock [61], here the role of photoelectrons is reduced to collecting these atoms into compact groups around the photosensitivity center at which this electron is localized. The electron's electric field polarizes the surrounding silver atoms, which acquire a dipole moment as a result. As is known, a dipole is drawn into the region with a stronger field, i.e. in this case it approaches the localized electron. The drift velocity is proportional to the mobility of the silver atoms, which rises with temperature. This increases the effectiveness of formation of latent-image centers. But, at the same time, this leads to an increase in the rate of spontaneous formation of similar groups of silver atoms, i.e. fogging (a factor mentioned earlier).

Photographic materials containing compounds of metals of different valences ($AgNO_3$, CsCl, $CdBr_2$, $Pb(NO_3)_2$, $HAuCl_4$) have also been studied [62–65]. The fraction of metal impurities introduced into the emulsions amounted to 0.01 mol per mole of photoemulsion silver. The materials were exposed at $T = 100$ °C, and the reference samples were the photographic materials (plates) exposed at 20 °C.

The results of these studies (see Fig. 4) show that the injection into the surface of AgHal crystals of impurities in the form of compounds of metals of different valences increases the integral sensitivity of the layer (with increasing temperature) in proportion, to the first approximation, to the valence of the metal in the chemical compounds used. The observed increase in the sensitivity is incomparably larger than the one obtained in Ref. [59] for photosensitive layers without impurities. The relatively large increase in sensitivity caused by a rise in temperature at the moment of exposure makes it possible to assume that the binding energy of the valence electrons in the impurity excited by light is not large. This is possible only if the light transforms the impurities into hydrogen-like systems, in which the binding energy decreases by a factor of ε^2 in comparison to the binding energy in unexcited impurities (ε is the dynamic dielectric constant of AgBr). The spectral response of the photographic materials under investigation increases with temperature if the impurities injected into the material contain metals of elevated valence [60]. The peaks on the curves *3* (see Fig. 4) give an idea of the photons whose energies are most effective in the process of simultaneous sensitization of the photosensitive materials by raising the temperature and injecting impurities. The peak corresponding to $\lambda \sim 350$ nm indicates that the photons have freed electrons from the halogen ions in the main substance, since the energy of these photons is almost the same as the electron affinity of the Br atom ($\sim 3.4-3.6$ eV). The peak corresponding to $\lambda = 400$ nm points to the existence of a band-to-band transition whose energy E_g is 3.05 eV at room temperature.

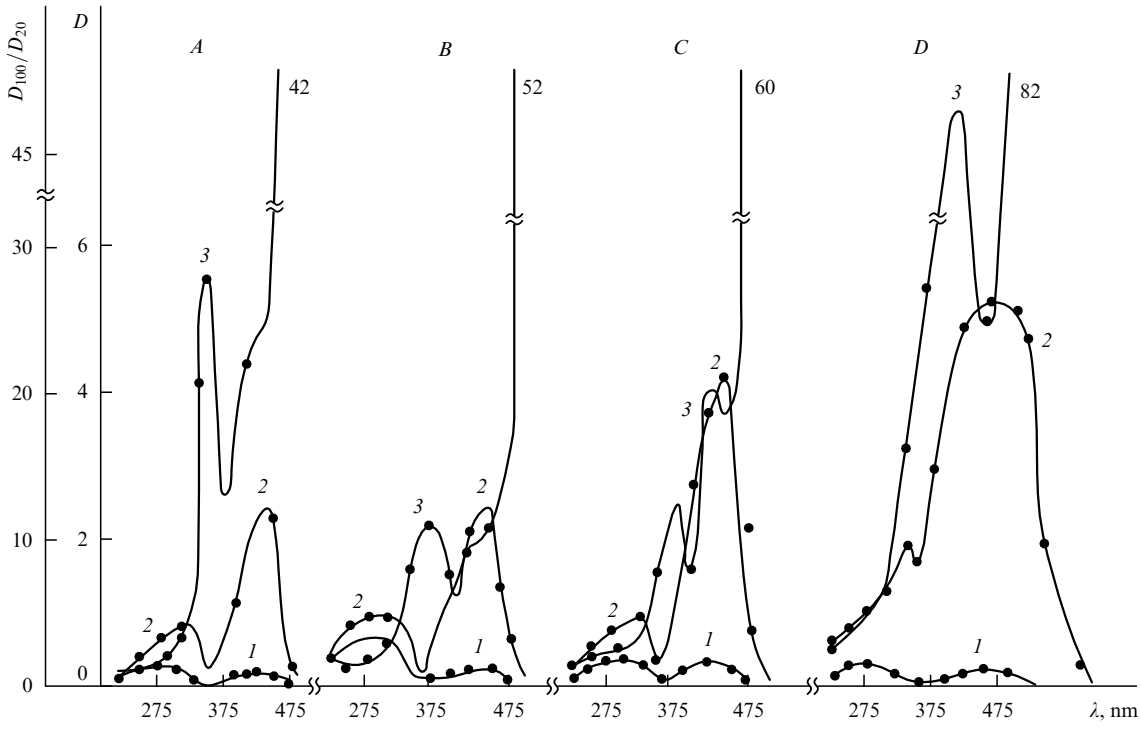

Figure 4. Dependence of the optical density of developed photosensitive materials with $AgNO_3$ (*A*), CsCl (*B*), $Pb(NO_3)_2$ (*C*), and $HAuCl_4$ (*D*) as impurities on the light's wavelength at 20 °C (curves *1*) and 100 °C (curves *2*) at the moment of exposure; curves *3* depict the relative variation of the optical density of the developed layer.

Thus, simultaneous raising the temperature of, and injecting impurities into, fine microcrystals of photochemical light indicators based on silver halides may be considered an effective way to increase their light sensitivity.

Studies of heavy-metal compounds showed that injection of some of the metals into the emulsion increased the emulsion's sensitivity (the developed image density was found to increase), and that this increase becomes noticeable even at room temperature. This effect is measurable when the amount of metal compounds is substantial compared to the amount of silver in the photographic material. Among the various effects of heavy-metal compounds on photographic materials we would like to point out the effect of sodium tungstate (Na_2WO_4) on the process of image formation in silver halide photographic materials [65 – 67].

Table 11 lists the results of tests of two kinds of industry-standard photoemulsions. We see that the photographic properties of these emulsions (containing sodium tungstate compounds) improve substantially as the silver content in the layer decreases from 4.70 g m^{-2} in the reference samples to 3.03 g m^{-2} in the transparency plates and from 5.43 g m^{-2} in the reference sample to 3.56 g m^{-2} in the reproduction plates: there is a 50% increase in photosensitivity, and also a 20% increase in the covering power in the transparency plates and a 50% increase in the covering power in the reproduction plates; the fog density and resolving power remained the same.

Table 11. Comparison of the characteristics of photosensitive materials: reference samples and samples with sodium tungstate as an addition (developer No. 1).

Characteristic	Transparency plates							
	Reference				With sodium tungstate			
	Developing time, min							
	3	4	5	6	3	4	5	6
$S_{0.2}$, GOST units	0.65	0.70	0.70	0.73	1.0	1.1	1.1	1.1
$S_{0.85}$, GOST units	3.2	3.7	3.7	3.8	4.5	5.0	5.5	5.5
γ	3.7	4.0	4,0	4.0	3.6	4.0	4.0	4.0
D_0	0.07	0.05	0.05	0.5	0.05	0.05	0.05	0.06
D_{max}	2.12	2.50	2.7	2.7	2.67	2.82	2.86	2.92
R, mm^{-1}	240				240			
Ag buildup, g m^{-2}	4.70				3.03			
Covering power	1.10				1.36			
Characteristic	Reproduction plates							
	Reference				With sodium tungstate			
	Developing time, min							
	4	6	8	10	4	6	8	10
$S_{0.2}$, GOST units	0.95	1.6	1.7	1.6	1.3	1.5	1.8	1.8
$S_{0.85}$, GOST units	5.0	8.7	9.5	9.5	8.5	10.0	11.0	11.0
γ	4.0	4.0	4,0	4.0	4.0	4.0	4.0	4.0
D_0	0.06	0.06	0.07	0.07	0.05	0.05	0.05	0.05
D_{max}	3.0	3.0	3.0	3.0	3.0	3.0	3.0	3.0
R, mm^{-1}	260				260			
Ag buildup, g m^{-2}	5.43				3.56			
Covering power	0.98				1.49			

Table 12 lists the photographic properties of transparency and reproduction photographic plates (reference samples and samples with a content of tungsten compounds) after expedited ageing (up to nine days) at 50 °C and 65% humidity. The results show that the ageing of the reference photographic materials and materials containing sodium tungstate compounds proceeds in the same way and without anomalies.

Figure 5 depicts the results of studies of laboratory-standard photoemulsions with a high resolving power, namely, reference samples and emulsions into which sodium tungstate had been injected. The curves show that as the silver content in the photoemulsion is reduced by a factor of three, the blackening density increases by a factor of 1.5 (curves *1* and *3*), while for equal silver content the increase is by a factor of three for emulsions containing tungsten compounds (curves *2* and *3*).

Table 13 lists the main characteristics of a photographic material with a high resolving power (the reference material) and a material in which 80% of the haloid silver is replaced by sodium tungstate. We see that as the silver content was reduced from 9 to 1.5 g m^{-2}, the photographic properties of the material even improved (the photosensitivity increased, while the other parameters remained the same).

Table 14 lists the photographic properties (and thus shows the changes in these properties) of a number of photoemulsions manufactured at the Moscow Industrial Photoplate Plant (abbreviated MZTF in Russian) and poured onto glass with sodium tungstate in a laboratory at the Russian Research Centre 'Kurchatov Institute', and Table 15 illustrates the properties of an MR-type nuclear photographic material in which 80% of silver halide is replaced by sodium tungstate. The glass onto which the photoemulsions were poured was 50-μm thick. The sensitivity was determined by the total blackening from exposing the emulsion to $Tl^{204}(\beta)$

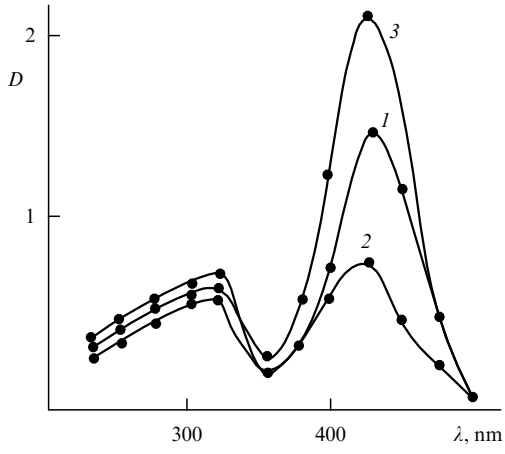

Figure 5. Dependence of the optical density on the wavelength of the light to which a photoemulsion with a high resolving power is exposed: *1*, the reference sample with 12-g m^{-2} silver content; *2*, an emulsion diluted by water so that the silver content is 4 g m^{-2}, and *3*, the same emulsion containing sodium tungstate, with 4-g m^{-2} silver content.

Table 12. Characteristics of the photographic properties of plates after expedited ageing at 50 °C and 65% humidity*.

Characteristic	Reference samples			Samples with sodium tungstate		
	Storing time, day					
	1	3	9	1	3	9
	Transparency plates					
$S_{0.2}$, GOST units	0.65	0.70	0.75	1.0	1.1	1.0
$S_{0.85}$, GOST units	3.3	3.4	2.4	4.8	5.0	4.5
γ	3.2	3.6	2.4	3.1	2.9	2.8
D_0	0.05	0.05	0.07	0.07	0.06	0.07
	Reproduction plates					
$S_{0.2}$, GOST units	1.7	1.8	1.4	2.5	2.9	3.1
$S_{0.85}$, GOST units	9.5	8.5	7.0	11	14	14
γ	4.0	4.0	4.0	4.0	4.0	4.0
D_0	0.07	0.09	0.09	0.06	0.09	0.10

* Developer No. 1; the transparency plates were developed for 5 min, and the reproduction plates for 8 min.

Table 13. Comparison of the characteristics of a photographic material used in holography: the reference sample, and a sample with sodium tungstate as an addition.

Characteristic	Reference sample	Sample with 80% of silver replaced by sodium tungstate
$S_{0.85}$, GOST units	0.10	0.15
γ	6	6
D_{max}	3.0	3.0
D_0	0.06	0.06
R, mm^{-1}	3000	3000
Ag buildup, $g\,m^{-2}$	9	1.5

radiation. Clearly, the reduction of the silver contents in the layer by a factor of 2.5 did not worsen the properties of the photographic material. Similar results were obtained when electrons with an energy in the 15–30-keV range were registered. When corpuscular radiation is registered, there appear certain limitations on the replacement of silver halides with sodium tungstate, related to the nature and energy of the particles being registered.

Silver halide photographic materials containing sodium tungstate exhibit, under an elevation of their temperature at the moment of exposure, a substantial increase in the developed optical density over the entire range of light waves from 225 to 525 nm [62]. We discovered such a phenomenon earlier in photographic materials that contained no salts of metals and in photosensitive materials with compounds of lead and cadmium injected into them.

When a photosensitive layer containing sodium tungstate was heated to 115 °C and exposed to light, the optical density was found to increase in comparison to the value for the same material at 20 °C for light of various wavelengths $\lambda = 325$, 350, 375, 400, and 475 nm according to the ratio D_{115}/D_{20} equal to 50, 11, 15.5, 15, and 20, respectively.

In photographic materials containing sodium tungstate, the fog density D_0 was the same as in the reference samples (see Tables 13–15).

After prolonged natural storage (for 6 to 12 months and more) it was found that, in the absence of antifogging measures, the fog density in layers containing sodium tungstate increased in relation to the silver content in the layers. Apparently, sodium tungstate in this case serves as a catalyst in the process of decomposition of silver compounds.

After prolonged storage at reduced temperatures or with antifogging measures carried out, photosensitive layers with sodium tungstate exhibit only a relatively small change in the fog density.

The photographic process of image production involving silver halide photographic materials consists of three stages: preparation of the emulsion, exposure, and chemicophoto-

Table 14. Characteristics of the photographic properties of the Mikrat NK, Mikro, and ÉS emulsions and negatives manufactured at MZTF with the ordinary amount of silver content (a), and with the silver content reduced by 50% (b) with sodium tungstate as an addition *.

Characteristic	Type of photographic emulsion							
	Mikrat NK		Mikro		Negative		ÉS **	
	a	b	a	b	a	b	a	b
$S_{0.1}$, GOST units	1.0	1.8	30	38	90	112	2.8	4.2
γ	5.3	8.5	2.3	2.3	0.8	0.9	2.2	2.1
D_{max}	1.88	> 3	> 3	> 3	1.62	1.66	2.5	2.5
D_0	0.10	0.10	0.06	0.06	0.08	0.08	0.06	0.08
Ag buildup, $g\,m^{-2}$	8.0	4.0	11.0	5.5	9.0	4.5	5.5	2.75

* All samples were developed in the standard No. 1 developer; the Mikrat NK and the Mikro emulsions were developed for 5 min, and the others for 4 min.

** Photosensitivity meets the $D_{0+0.9}$ criterion.

Table 15. Comparison of the characteristics of a photosensitive material of the MR type, used in recording corpuscular radiation: the reference sample, and a sample with sodium tungstate as an addition.

Characteristic	Reference sample	Sample with 60% of silver replaced by sodium tungstate
Sensitivity (blackening density) to Tl^{204} radiation	0.40	0.45
D_0		
R, mm^{-1}	0.06	0.06
Ag buildup, g m^{-2}	240	240
	30	12

graphic processing. The effect of sodium tungstate on each has been thoroughly studied. Some experiments have shown that the presence of sodium tungstate is important only in one stage — exposure. In the first series of experiments, sodium tungstate was injected at the stage of preparing the emulsion for pouring onto the substrate; then the sodium tungstate was washed out, and the material was exposed. In the second series, the photographic plates with sodium tungstate were first exposed and then the sodium tungstate was washed out. In the third series, the reference plates were exposed and only after that a solution of sodium tungstate was applied to them. In all three series the samples were developed in the same way. It was found that sodium tungstate had an effect only in the second series, when it was present during the exposure stage.

Below we summarize the main experimental facts obtained in the process of studying the effect of sodium tungstate on silver halide photographic materials [66, 68].

(1) The photolysis of photographic materials containing sodium tungstate proceeds much faster than the photolysis of the reference photographic material that contains no sodium tungstate.

(2) The induction period in the developing process is shorter for materials containing sodium tungstate.

(3) The optical density of a developed photosensitive layer containing sodium tungstate and silver bromide is higher than that of a photosensitive layer with the same silver bromide content but without sodium tungstate.

(4) The amount of developed silver in materials containing sodium tungstate is approximately twice as great as in the reference samples, i.e. the presence of sodium tungstate on the surfaces of silver halide microcrystals promotes the development of a larger number of such crystals, which attests to the greater efficiency of the silver employment in the presence of sodium tungstate.

(5) That the optical density of the developed image in a photosensitive layer containing sodium tungstate is higher than the value in a photosensitive layer not containing sodium tungstate is evident for the entire spectral-response range (250 – 500 nm) studied so far.

(6) No selective spectral sensitization of photoemulsions in the range of wavelengths from 250 to 1000 nm, caused by the injection of sodium tungstate, has been observed.

(7) The aqueous solution of sodium tungstate has an alkaline reaction, so that injection of sodium tungstate into an emulsion increases the pH of this emulsion. However, the contribution of this increase in pH to the increase in sensitivity is moderate. Comparative studies of properties of emulsions that acquire the same pH when a solution of sodium tungstate or an alkali (NaOH and KOH) is added have shown that in all cases mentioned in items 1 to 5 the effect is much heightened when the solution of sodium tungstate is present.

(8) The injection of sodium tungstate into photographic emulsions improves the properties of such emulsions (or at least does not worsen them) with a substantial decrease in the silver content (Figs 5 and 6).

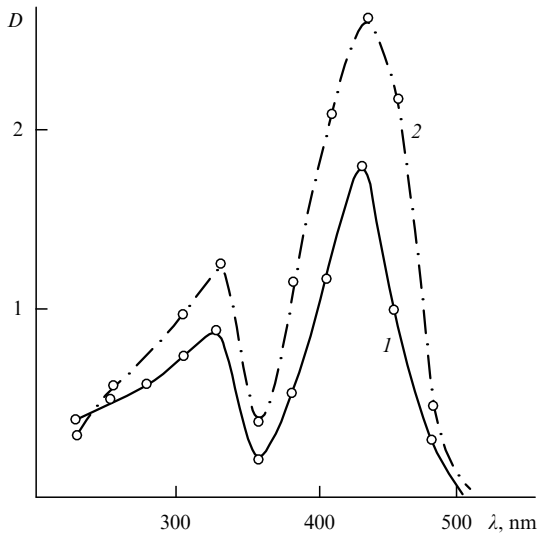

Figure 6. Dependence of the optical density on the wavelength of the light to which photosensitive emulsions are exposed: *1*, the reference emulsion with a silver content of 9 g m^{-2}, and *2*, the same emulsion diluted by a solution of sodium tungstate to a silver content of 2.25 g m^{-2}.

(9) Electron microscopy studies of emulsions containing sodium tungstate have shown that there are no visible changes in the silver halide microcrystals as compared to the reference emulsion (Fig. 7), except for the fact that an electron beam more rapidly decomposes silver halide crystals with sodium tungstate compared to such crystals without sodium tungstate. Neither were there observed any changes in developed crystals.

(10) Electron microscopy studies also showed that there is no additional electron diffraction on silver halide microcrystals of the emulsion containing sodium tungstate, thus proving that sodium tungstate crystals simply do not exist.

The very fact that the presence of sodium tungstate has an effect only in the exposure process could have been connected to the ordinary sensitization effect of Na_2WO_4 on silver halides, but additional experiments have shown that in our conditions the sensitization mechanism does not operate. First, the injection of Na_2WO_4 into a photoemulsion in the amounts comparable to those of ordinary chemical or optical sensitizers (gold thiocyanate, sulfurous sensitizers, dyes, etc.) has no positive effect. For such an effect to emerge, the amount of Na_2WO_4 must be 0.3 – 0.5 g for each gram of metallic silver. Second (and this is the most important factor), the light absorption by a solution of sodium tungstate in the wavelength range under investigation (250 – 1000 nm) is practically nil, and for the sensitization mechanism to operate the sensitizer's absorption spectrum must have fairly high peaks.

The above investigations show that the effect of sodium tungstate on the process of formation of developing centers in silver halide photographic materials is, from the viewpoint of physics, a new one. Its mechanism cannot be justified if one

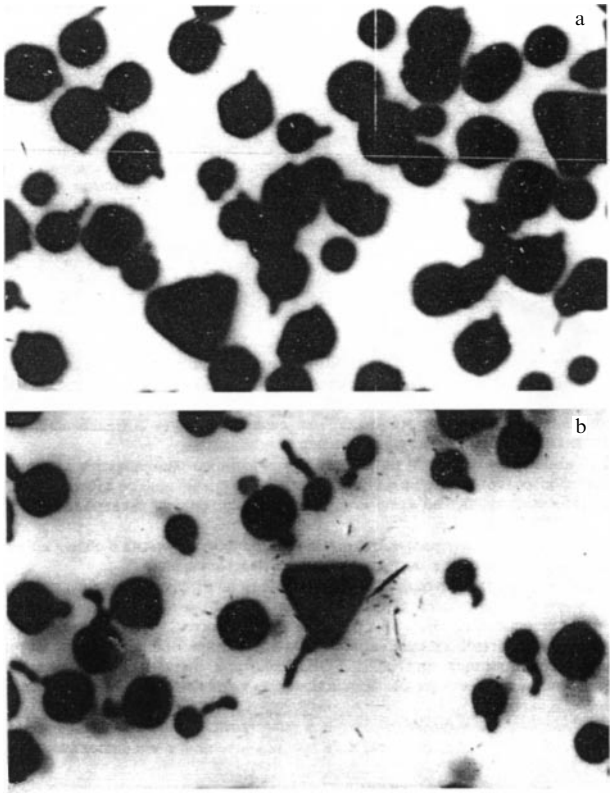

Figure 7. Electron micrographs of AgHal microcrystals of a reference positive emulsion (a), and of the same emulsion containing sodium tungstate (b).

remains within the common realm of physicochemical mechanisms that operate in processes of optical or chemical sensitization. As noted earlier, the necessary condition for optical sensitization to occur is the presence in the sensitizer's absorption spectrum of bands or peaks, while for the solution of sodium tungstate the absorption of light over the entire visible range of wavelengths is practically nil. At the same time, a characteristic feature of chemical sensitization processes (say, in the case of gold sensitization) is that the metallic Au and Ag are isomorphic and that the atomic and ionic radii of silver and the sensitizer are almost the same. In our case these conditions are not met.

Photographic materials treated with sodium tungstate retain their high photosensitivity even if the silver halide content is reduced. Such behavior is corroborated by the fact that attaining the same optical densities requires much less energy of the same spectral composition when the emulsion contains sodium tungstate. Hence, the quantum yield of the entire process of latent-image formation, equal to the ratio of the number of photoelectrons N_{photoel} used in the formation of latent-image silver to the number of absorbed photons N_{abs}, where $N_{\text{abs}} = N_{\text{inc}} - (N_{\text{refl}} + N_{\text{trans}})$, is much higher in the case where the light acting on the surface of AgHal microcrystals containing sodium tungstate produces a substantial amount of photolytic silver, i.e.

$$\eta = \frac{N_{\text{photoel}}}{N_{\text{abs}}} > \eta_{\text{refer}} = \frac{N_{\text{refer. photoel}}}{N_{\text{refer. abs}}} .$$

We assume that under the same experimental conditions the optical density is proportional to η, so that $D/D_{\text{refer}} = \eta/\eta_{\text{refer}}$.

The curves in Fig. 8 are similar to the above data on the effect of heavy-metal compounds at elevated temperatures in silver halide photographic materials (see Table 8).

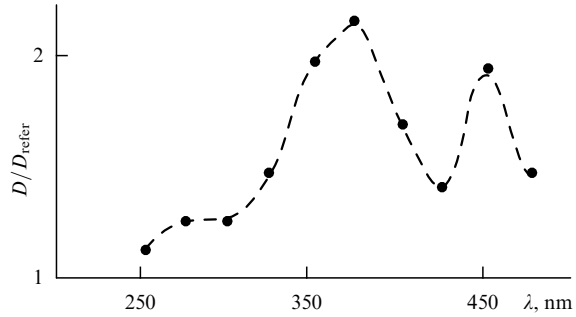

Figure 8. Dependence of the ratio of the optical density of a developed high-resolution emulsion diluted with a solution of sodium tungstate (to a silver content of 2.25 g m^{-2} in the photographic plates) to that of the reference emulsion (with a silver content of 9 g m^{-2}) on the wavelength of the light to which the emulsions were exposed.

Here we are probably dealing with the catalytic effect of sodium tungstate on AgHal microcrystals. In other words, as a result of the interaction of the complex $(WO_4)^{2-}$ and the silver ions on the surface of AgHal, light or charged particles initiate the intense formation of silver atoms followed by the formation of developing centers.

The above implies that a rise in the temperature of the investigated photographic materials at the moment of exposure increases their sensitivity.

We have also showed that it is possible to substantially reduce the silver content in silver halide photographic materials and still retain the properties of these materials by injecting sodium tungstate into the photoemulsion. This method will make it possible to save about 30% of the silver in some photographic materials with the sensitivity of these materials remaining unchanged.

4. Conclusions

The spectra of light absorption, luminescence, and photographic (photochemical) and photoelectric sensitivities and the exciton binding energies in the photosensitive crystals AgHal, AuHal, TlHal, and $PbHal_2$ are connected by regularities characteristic of hydrogen-like systems in these crystals.

The quantities determined for one of the crystals can be applied to the other crystals by using the correction factor $\varepsilon_2^2/\varepsilon_1^2$.

The positions of the maxima of the absorption band and lines, the photocurrent, the photosensitivity, and the luminescence lines on the spectral characteristics of these crystals are described by modified equations of the theory of large-radius excitons (Wannier – Mott excitons).

Each energy level of a Wannier – Mott exciton is the boundary of a series of lines.

The author would like to express his gratitude to R V Ryabova for her collaboration in a number of experiments described in Section 3.

References

1. Ryzhanov S G *Zh. Eksp. Teor. Fiz.* **15** 108 (1945)
2. Ryzhanov S G *Zh. Nauch. Prikl. Foto- i Kinematografii* **3** (1) 3 (1958); **12** (1) 61 (1967)
3. Barshchevskiĭ B U *Fiz. Tverd. Tela* (Leningrad) **10** 3689 (1968); **11** 2745 (1969)
4. Barshchevskiĭ B U *Fotoélektricheskie i Opticheskie Svoĭstva Galogenidov Serebra* (Photoelectric and Optical Properties of Silver Halides) (Moscow: Izd. VZIITa, 1967)
5. Kozyreva E B, Meĭklyar P V *Opt. Spektrosk.* **23** 421 (1967)
6. Ryzhanov S G *Opt. Spektrosk.* **17** 294 (1964)
7. Lider K F, Novikov B V *Vest. Leningrad. Gos. Univ.* (10) 46 (1963)
8. Aline P G *Phys. Rev.* **105** 406 (1957)
9. Kirillov E A, Fomenko A C *Tr. OGU. Sbornik Fiz.–Mat. Fakul'teta i NII Fiz.* **3** 7 (1951)
10. Brown F C, Masumi T, Tippins H H *J. Phys. Chem. Solids* **22** 101 (1961)
11. Barshchevskiĭ B U *Fiz. Tverd. Tela* (Leningrad) **12** 906 (1970)
12. Perny G *J. Chem. Phys.* **55** 651 (1958); **57** 17 (1960)
13. Barshchevskiĭ B U, Ryabova R V *Dokl. Ross. Akad. Nauk* **332** (5) 585 (1993)
14. Kanzaki H, Sakuragi S, Sakamoto K *Solid State Commun.* **9** 999 (1971); **9** 1667 (1971)
15. Moser F, van Heyningen R S, Lyu S *Solid State Commun.* **7** 1609 (1969)
16. Höhne M, Stasiw M *Phys. Status Solidi* **28** 247 (1968)
17. Meidinger W *Fortschr. Photographie* **3** 1 (1944) [Translated into Russian, in *Khimiya Fotograficheskikh Protsessov* (The Chemistry of Photographic Processes) (Ed. B U Barshchevskiĭ) (Moscow: IIL, 1951) p. 58 [a collection of translations into Russian of various papers on the subject]]
18. Golub S I *Usp. Nauch. Fotografii* **1** 205 (1951)
19. Belous V M, Golub S I *Izv. Vyssh. Uchebn. Zaved. Fiz.* (1) 89 (1963)
20. Barshchevskiĭ B U et al. *Dokl. Akad. Nauk SSSR* **213** 627 (1973)
21. Barshchevskiĭ B U, Safronov G M *Dokl. Akad. Nauk SSSR* **218** 1124 (1974)
22. Barshchevskiĭ B U *Dokl. Akad. Nauk SSSR* **208** 627 (1973)
23. Kanzaki H, Sakuragi S *J. Phys. Soc. Jpn.* **27** 109 (1969)
24. Kozyreva E B *Opt. Spektrosk.* **25** 526 (1968)
25. Golub S I, Orlovskaya N A *Izv. Akad. Nauk SSSR Ser. Fiz.* **25** 388 (1961)
26. Moss T S *Optical Properties of Semiconductors* (London: Butterworths Sci. Publ., 1959) [Translated into Russian (Moscow: IIL, 1961) p. 62]
27. Barshchevskiĭ B U, Batog B N, Safronov G M *Dokl. Akad. Nauk SSSR* **208** 608 (1973); **197** 1100 (1971)
28. Silukova T N, in *Tr. Latvian Gos. Univ. NII Fiz. Tverd. Tela* (1980) p. 168
29. Tutihasi S *J. Phys. Chem. Solids* **12** 344 (1960)
30. Boldyrev V V *Zh. Nauch. Prikl. Foto- i Kinematografii* **19** (2) 91 (1974)
31. Élmas R, Kink R *Tr. Inst. Fiz. Astron. Akad. Nauk. Ést. SSR* **26** 112 (1964)
32. Lidja G G, Plekhanov V G, Malysheva A A *Izv. Akad. Nauk Ést. SSR* **19** (3) 328 (1970)
33. Lidja G, Plekhanov V G, Preprint FAJ-17 (Tartu: Inst. of Phys. and Astronom. Akad. Sci. Est. SSR, 1972)
34. Lidja G G, Dobrzhanskiĭ G F, Plekhanov V G *Tr. Inst. Fiz. Astron. Akad. Nauk Ést. SSR* **39** 63 (1972)
35. Plekhanov V G, Lidja G G *Izv. Akad. Nauk SSSR* **38** (6) 1304 (1974)
36. Lidja G G, Plekhanov V G *Izv. Akad. Nauk Ést. SSR* **21** (2) 193 (1972)
37. Kink R et al., in *Tr. Inst. Fiz. Astron. Akad. Nauk Ést. SSR* **36** (1969)
38. Belous V M et al. *Zh. Nauch. Prikl. Foto- i Kinematografii* **23** (6) 460 (1978)
39. Fowler W B *Phys. Rev.* **151** 657 (1966)
40. Saint-James D *J. Phys. Et. Rad.* **18** 260 (1957)
41. Yagi H *J. Phys. Soc. Jpn.* **11** 430 (1956) [Translated into Russian, in *Tsentry Okraski v Shchelochnogaloidnykh Kristallakh* (Color Centers in Alkali–Halide Crystals) (Moscow: IIL, 1958) p. 125 [a collection of translations into Russian of various papers on the subject]]
42. Barshchevskiĭ B U, Gurevich Yu A *Dokl. Akad. Nauk SSSR* **191** 115 (1970)
43. Barshchevskiĭ B U, Gurevich Yu A *Fiz. Tverd. Tela* (Leningrad) **12** 3380 (1970)
44. Savost'yanova M V *Usp. Fiz. Nauk* **22** 168 (1939)
45. Miyata T *J. Phys. Soc. Jpn.* **31** 529 (1971)
46. Almazov A B 'Ionnye radiusy' ('Ionic radii'), in *Fizicheskiĭ Entsiklopedicheskiĭ Slovar'* (Physics Encyclopedic Dictionary) Vol. 2 (Eds B A Vvedenskiĭ et al.) (Moscow: Sovetskaya Entsiklopediya, 1962) p. 232
47. Barshchevskiĭ B U *Dokl. Akad. Nauk SSSR* **65** 125 (1949)
48. Leĭbzon S A et al. *Zh. Nauch. Prikl. Foto- i Kinematografii* **18** 469 (1973)
49. Barshchevskiĭ B U *Tr. Vsesoyuz. Zaoch. Inst. Inzhenerov Transporta* **62** 42 (1972)
50. Barshchevskiĭ B U, Trekhov E S *Kolloid. Zh.* **36** (1) 9 (1974)
51. Ryabova R V, Barshchevskiĭ B U, Myatezh O V *Dokl. Ross. Akad. Nauk* **349** 493 (1996)
52. Barshchevskiĭ B U, Leĭbzon S A, Uvarova V M, Sheberstov V I, Shpol'skiĭ M R, Larin G M *Zh. Fiz. Khim.* **49** 348 (1975)
53. Sablin-Yavorskiĭ A D, Vigant V V, Fridkin V M *Zh. Nauch. Prikl. Foto- i Kinematografii* **18** 389 (1973)
54. Barshchevskiĭ B U *Fiz. Tverd. Tela* (Leningrad) **11** 2745 (1969); **12** 906 (1970)
55. Barshchevskiĭ B U *Dokl. Akad. Nauk SSSR* **19** 1100 (1971)
56. Korotaev N N, Meĭklyar P V, in *Dokl. Mezhdunar. Kongr. po Fotogr. Nauke* (Reports at Int. Congr. on Photography Sci.) Sect. AB (Moscow: VTI, 1970) p. 102
57. Mees C E K, James T H (Eds) *The Theory of the Photographic Process* (New York: MacMillan Co., 1966) [Translated into Russian (Leningrad: Khimiya, 1973) p. 34]
58. Deb S K *Phys. Rev. B* **2** 5003 (1970)
59. Barshchevskiĭ B U, Kondrashina A A, Ryabova R V *Zh. Fiz. Khim.* **52** 2406 (1978)
60. Barshchevskiĭ B U, Gromova B P, Kondrashina A A, Ryabova R V *Zh. Fiz. Khim.* **51** 2336 (1977)
61. Galashin E A, Fock M V *Zh. Nauch. Prikl. Foto- i Kinematografii* **17** 559 (1972)
62. Barshchevskiĭ B U, Kondrashina A A, Ryabova R V, USSR Author's Certificate No. 697957; *Byull. Izobret.* No. 42 (Moscow: VINITI, 1979)
63. Barshchevskiĭ B U, Kondrashina A A *Dokl. Akad. Nauk SSSR* **242** 1375 (1978)
64. Ryabova R V, Barshchevskiĭ B U, Kondrashina A A *Dokl. Akad. Nauk SSSR* **306** 142 (1989)
65. Barshchevskiĭ B U, Kondrashina A A, Ryabova R V, USSR Author's Certificate No. 1192512; *Byull. Izobret.* No. 2 (Moscow: VINITI, 1985)
66. Ryabova R V, Barshchevskiĭ B U, Kondrashina A A, Lomonosov V V *Dokl. Akad. Nauk SSSR* **315** 409 (1990)
67. Barshchevskiĭ B U *Usp. Nauch. Fotografii* **1** 191 (1951)
68. Barshchevskiĭ B U, Ryabova R V *Zh. Nauch. Prikl. Foto- i Kinematografii* **45** 44 (1998)